DEPARTMENT OF THE AIR FORCE
AIR UNIVERSITY

AIR FORCE INSTITUTE OF TECHNOLOGY

Wright-Patterson Air Force Base, Ohio

AFIT/GA/ENY/90D-14

A NUMERICAL INVESTIGATION OF THE SERIES REVERSION/INVERSION AND SERIES REVERSION OF LAMBERT'S TIME FUNCTION

THESIS

Michael P. Ward
Captain, USAF

AFIT/GA/ENY/90D-14

Approved for public release; distribution unlimited

AFIT/GA/ENY/90D-14

A NUMERICAL INVESTIGATION OF THE SERIES REVERSION/INVERSION AND SERIES REVERSION OF LAMBERT'S TIME FUNCTION

THESIS

Presented to the Faculty of the School of Engineering
of the Air Force Institute of Technology
Air University
In Partial Fulfillment of the
Requirements for the Degree of
Master of Science in Astronautical Engineering

Michael P. Ward, B.S.
Captain, USAF

December, 1990

Approved for public release; distribution unlimited

Acknowledgments

I would like to thank my advisor, Capt Rodney Bain, for all of his help and expert guidance. A special thanks are due to my wife, Laura for her patience and understanding during this degree program and to my son, Christopher, for providing the necessary "baby breaks".

Michael P. Ward

Table of Contents

List of Figures

List of Tables

List of Symbols

Abstract

An expression for the semi-major axis as a function of time may be determined by performing a series reversion and inversion of Lambert's Time Function. Since the resulting series contains a singularity, it is desirable to perform only a reversion on the original series to obtain an expression for the inverse of the semi-major axis. Using a Lagrange expansion to obtain the coefficients for this series is very computer intensive. Therefore, alternative methods are presented. Also, each series was expanded into a continued fraction which provided greater accuracy than the series using the same number of coefficients. The accuracy was found to be dependent upon the number of series coefficients used, the transfer time, and the transfer angle.

A NUMERICAL INVESTIGATION OF THE SERIES REVERSION/INVERSION AND SERIES REVERSION OF LAMBERT'S TIME FUNCTION

I. Introduction

One of the classic problems in orbital mechanics is the determination of orbital parameters using two position vectors and the time of flight of a satellite. In 1761, Lambert developed a theorem (later proved by Lagrange) which states the time to traverse an elliptic arc (also true for any conic trajectory (2:/)) is dependent only on the semi-major axis, the perimeter of the triangle formed by the initial and final position vectors, and the chord joining the initial and final points of the arc. The geometry is shown in Figure 1. Throughout this research the radius vectors were held constant, $r_1 = r_2 = 1$ au and the transfer angle was varied from 10 to 360 degrees.

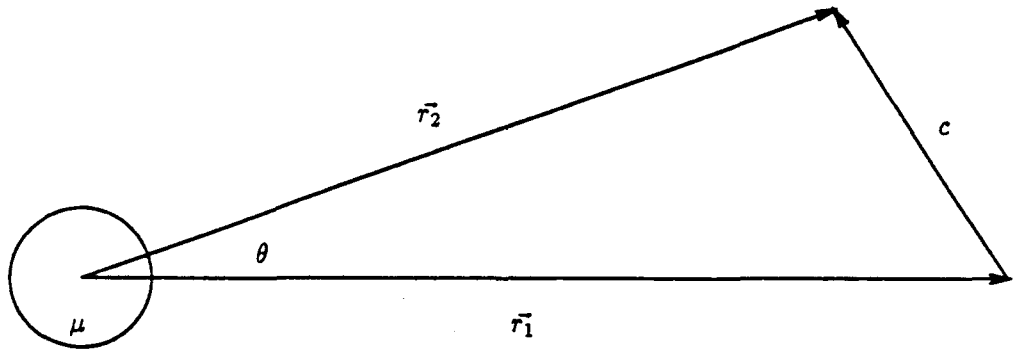

Figure 1. Geometry of Lambert's Theorem

The significance of Lambert's theorem can be seen in Figure 2. Consider the elliptic arc joining the fixed points P and Q. According to Lambert's theorem the shape of the transfer ellipse from P to Q may be altered without changing the time of flight by moving the foci F and F^* and keeping the semi-major axis constant. Therefore, the focus F may be moved to F_1 and the focus F^* to F_1^* without changing the time of flight.

As the focus F is moved counterclockwise and the focus F^* is moved clockwise, the ellipse becomes very flat until the foci are at F_2 and F_2^*. The time of flight has not changed and the orbit is now rectilinear. Thus, the time t may be computed by elementary methods.

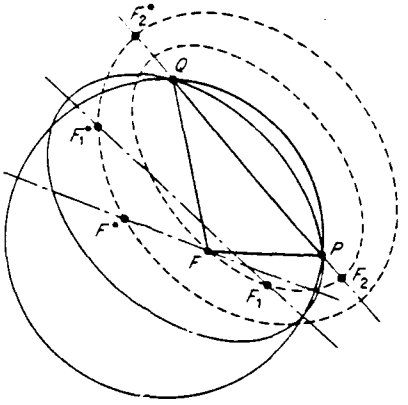

Figure 2. Geometrical Significance of Lambert's Theorem (2:72)

To obtain Lambert's Time Function the energy equation for a two-body orbit may be written as

$$\left(\frac{dr}{dt}\right)^2 = \mu\left(\frac{2}{r} - \frac{1}{a}\right) \tag{1}$$

where r is the radial distance between the two bodies, μ is the gravitational constant, a is the semi-major axis, and t is the time. Since

$$QF_2 + PF_2 = r_1 + r_2 \quad \text{and} \quad QF_2 - PF_2 = c$$

then

$$PF_2 = s - c \quad \text{and} \quad QF_2 = s$$

where $s = (r_1 + r_2 + c)/2$. Integrating Eq (1) produces

$$t = \frac{1}{\sqrt{\mu}} \int_{s-c}^{s} \frac{r\,dr}{\sqrt{2r - r^2/a}} \tag{2}$$

Employing the following change of variable:

$$r = a(1 - \cos\phi)$$

Eq (2) may be written as

$$t = \sqrt{\frac{a^3}{\mu}} \int_{\beta}^{\alpha} (1 - \cos\phi) d\phi$$

where

$$\alpha = 2\sin^{-1}\sqrt{\frac{s}{2a}} \quad \text{and} \quad \beta = 2\sin^{-1}\sqrt{\frac{s-c}{2a}}$$

This produces

$$t = \sqrt{\frac{a^3}{\mu}}[(\alpha - \sin\alpha) - (\beta - \sin\beta)] \tag{3}$$

This is Lambert's Time Function for an elliptic trajectory with a transfer angle less than π and a flight time less than the minimum energy transfer time. A minimum energy transfer is an elliptical transfer where $a = s/2$. It may also be shown for a transfer angle greater than π Lambert's Time Function is given by

$$t = \sqrt{\frac{a^3}{\mu}}[(\alpha - \sin\alpha) + (\beta - \sin\beta)] \tag{4}$$

This form of Lambert's Time Function is difficult to use since the transfer time is often known and the semi-major axis is the parameter that needs to be determined. Since the equation is transcendental in the semi-major axis root finding techniques are employed in order to determine the semi-major axis. A method of expressing the semi-major axis as a function of the transfer time is desired.

With the use of hypergeometric functions, Lambert's Time Function for an elliptical trajectory may be written as an infinite series:

$$T = \left(\frac{t}{t_p} - 1\right) = \sum_{n=1}^{\infty} \frac{\left(1 - \left(\frac{s-c}{s}\right)^{n+3/2}\right)\left(\frac{1}{2}\right)_n \left(\frac{3}{2}\right)_n}{\left(1 - \left(\frac{s-c}{s}\right)^{3/2}\right)\left(\frac{5}{2}\right)_n n!}\left(\frac{s}{2a}\right)^n$$

$$= A_1\left(\frac{s}{2a}\right) + A_2\left(\frac{s}{2a}\right)^2 + A_3\left(\frac{s}{2a}\right)^3 + \ldots \tag{5}$$

where

$$t_p = \frac{2}{3}\sqrt{\frac{s^3}{2\mu}}\left(1 - \left(\frac{s-c}{s}\right)^{3/2}\right)$$

is the parabolic transfer time. This is the flight time of an object traveling on a parabolic trajectory between two position vectors where the origin of the position vectors is the focus of the parabola. Lambert's Time Function for a hyperbolic trajectory may also be expressed as an infinite series identical to Eq (5) except in the sign of the argument, i. e., $\left(-\frac{s}{2a}\right)$, and the series coefficients are identical.

A series reversion and inversion has been performed on Eq (5) in order to obtain the semi-major axis as a function of time (4:9-13):

$$\left(\frac{2a}{s}\right) = B_1 T^{-1} + B_2 T^0 + B_3 T^1 + B_4 T^2 + \ldots \tag{6}$$

The coefficients for this series, referred to as the RI series, are obtained using a numerically efficient matrix formulation. One purpose of this research is to investigate the accuracy of the RI series. Due to the existence of a singularity in the RI series at $T = 0$ it is desirable to perform only a series reversion on Eq (5) to obtain the inverse of the semi-major axis as a function of time:

$$\left(\frac{s}{2a}\right) = \alpha_1 T + \alpha_2 T^2 + \alpha_3 T^3 + \alpha_4 T^4 + \ldots \tag{7}$$

This series will be referred to as the R series. Several methods of obtaining the coefficients for the R series are presented as well as the accuracy of each method.

II. Analytical Development

Measuring the Accuracy

The accuracy of each method was evaluated in the following manner: 1) For a given geometry and transfer time a value for the semi-major axis was obtained using Eq (6) or (7) for a given number of terms; 2) The time was calculated from Eq (3) or (4) using the value for semi-major axis obtained in step 1; 3) The absolute value of the difference between the calculated time and the true time was then calculated. The value obtained in step 3 is called the Time Residual and was employed as a measure of the accuracy of each method.

Calculating the RI Series Coefficients

To calculate the coefficients for the RI series, multiply Eq (6) by $\left(\frac{s}{2a}\right)T$ to obtain:

$$T = B_1\left(\frac{s}{2a}\right) + B_2\left(\frac{s}{2a}\right)T + \dots \tag{8}$$

Substituting the series solution for T given by Eq (5) into Eq (8) yields:

$$A_1\left(\frac{s}{2a}\right) + A_2\left(\frac{s}{2a}\right)^2 + A_3\left(\frac{s}{2a}\right)^3 + \dots =$$

$$B_1\left(\frac{s}{2a}\right) + B_2\left(\frac{s}{2a}\right)\left\{A_1\left(\frac{s}{2a}\right) + A_2\left(\frac{s}{2a}\right)^2 + A_3\left(\frac{s}{2a}\right)^3 + \dots\right\} + \dots \tag{9}$$

Now differentiate Eq (9) with respect to $\left(\frac{s}{2a}\right)$ to obtain:

$$A_1 + 2A_2\left(\frac{s}{2a}\right) + 3A_3\left(\frac{s}{2a}\right)^2 + \dots =$$

$$B_1 + B_2\left\{A_1\left(\frac{s}{2a}\right) + A_2\left(\frac{s}{2a}\right)^2 + A_3\left(\frac{s}{2a}\right)^3 + \dots\right\} \tag{10}$$

$$+ B_2\left(\frac{s}{2a}\right)\left\{A_1 + 2A_2\left(\frac{s}{2a}\right) + 3A_3\left(\frac{s}{2a}\right)^2 + \dots\right\} + \dots$$

Evaluating Eq (10) at $\left(\frac{s}{2a}\right) = 0$ yields:

$$A_1 = B_1$$

Taking three more derivatives and evaluating each at $\left(\frac{s}{2a}\right) = 0$ produces the following:

$$A_2 = A_1 B_2$$

$$A_3 = A_2 B_2 + A_1^2 B_3$$

$$A_4 = A_3 B_2 + 2A_1 A_2 B_3 + A_1^3 B_4 \qquad (11)$$

Each successive derivative becomes increasingly more complex. Solving Equation set (11) for the B_i coefficients yields:

$$B_2 = \frac{A_2}{A_1}$$

$$B_3 = \frac{A_1 A_3 - A_2^2}{A_1^3}$$

$$B_4 = \frac{A_1^2 A_4 - 3A_1 A_2 A_3 + 2A_2^3}{A_1^5} \qquad (12)$$

Equation set (12) may be expressed in matrix form as:

$$\begin{Bmatrix} B_2 \\ B_3 \\ B_4 \\ . \\ B_{i+1} \end{Bmatrix} = \begin{bmatrix} \frac{1}{A_1} & 0 & 0 & 0 & 0 \\ \frac{-A_2}{A_1^3} & \frac{1}{A_1^2} & 0 & 0 & 0 \\ \frac{2A_2^2 - A_1 A_3}{A_1^5} & \frac{-2A_2}{A_1^4} & \frac{1}{A_1^3} & 0 & 0 \\ . & . & . & . & 0 \\ . & . & . & . & \frac{1}{A_1^i} \end{bmatrix} \begin{Bmatrix} A_2 \\ A_3 \\ A_4 \\ . \\ A_{i+1} \end{Bmatrix} = \mathbf{Q}\{A_n\} \qquad (13)$$

A method of generating the Q matrix in Eq (13) has been discovered (4:12). Knowing the elements of the first two rows of the matrix all of the remaining elements may be obtained using the following procedure:

1. $q_{11} = \frac{1}{A_1}$, $q_{21} = -\frac{A_2}{A_1^3}$, $q_{22} = \frac{1}{A_1^2}$

2. $q_{ij} = (q_{i-1,1}, q_{i-2,1}, \ldots, q_{11}) \cdot (q_{1,j-1}, q_{2,j-1}, \ldots, q_{i-1,j-1})$, $i \geq j > 2$
3. $q_{i1} = -\frac{1}{A_1}\{(q_{i2}, q_{i3}, \ldots, q_{in}) \cdot (A_2, A_3, \ldots, A_i)\}$
4. $B_{i+1} = (q_{i1}, q_{i2}, \ldots, q_{in}) \cdot (A_2, A_3, \ldots, A_{i+1})$

The first element of each row must be calculated last, since it is dependent upon all of the other elements in that row. For example, to calculate B_4 first form element q_{33}:

$$q_{33} = (q_{21}, q_{11}) \cdot (q_{12}, q_{22})$$

$$= \left(-\frac{A_2}{A_1^3}, \frac{1}{A_1} \right) \cdot \left(0, \frac{1}{A_1^2} \right) = \frac{1}{A_1^3}$$

then q_{32}:

$$q_{32} = (q_{21}, q_{11}) \cdot (q_{11}, q_{21})$$

$$= \left(-\frac{A_2}{A_1^3}, \frac{1}{A_1} \right) \cdot \left(\frac{1}{A_1}, -\frac{A_2}{A_1^3} \right) = -\frac{2A_2}{A_1^4}$$

then q_{31}:

$$q_{31} = -\frac{1}{A_1} \{ (q_{32}, q_{33}) \cdot (A_2, A_3) \}$$

$$= -\frac{1}{A_1} \left\{ -\frac{2A_2^2}{A_1^4} + \frac{A_3}{A_1^3} \right\} = \frac{2A_2^2 - A_1 A_3}{A_1^5}$$

Now that all of the elements of the third row are known, B_4 may be calculated by taking the dot product shown in step 4. Each successive coefficient may be calculated by repeating steps 2, 3, and 4. The first 26 coefficients for a transfer angle of 60 degrees are listed in Table 1.

TABLE 1: RI Series Coefficients for $\theta = 60°$

n	B_n
1	3.476627109438971E-001
2	5.601954800296930E-001
3	1.569332354004166E-001
4	-2.072127624535575E-002
5	1.341485080981992E-002
6	-9.591469176204521E-003
7	5.932190937546468E-003
8	-3.159031868854800E-003
9	1.491664314059560E-003
10	-6.607117824078135E-004
11	3.008808653647832E-004
12	-1.524580592486835E-004
13	8.421050704976452E-005
14	-4.626845621302778E-005
15	2.360695540204460E-005
16	-1.103113408618128E-005
17	4.944780755522515E-006
18	-2.408810757970059E-006
19	1.335338311037049E-006
20	-1.428209543519188E-006
21	-2.160844815080054E-006
22	2.140513606718741E-005
23	-1.160819447250105E-004
24	6.927153735887259E-004
25	-3.255901276133955E-003
26	1.382574881426990E-002

Calculating the R Series Coefficients

The coefficients for the R series may be obtained by using the Lagrange expansion theorem (1). Letting $x = \left(\frac{s}{2a}\right)$, Eq (5) may be written in the form:

$$x = x_0 + T\phi(x) \tag{14}$$

with $x_0 = 0$, where

$$\phi(x) = \frac{1}{A_1 + A_2 x + A_3 x^2 + \ldots} \tag{15}$$

and the A_n terms are the coefficients in Eq (5). Now x may be expressed as a power series in T using the Lagrange expansion theorem with the coefficients given by

$$\alpha_n = \frac{1}{n!}\frac{d^{n-1}}{dx^{n-1}}\phi(x)^n\Big|_{x=x_0}$$

The following recursive algorithm was used to calculate the coefficients of Eq (7) (3:212-215). Define

$$D_k^n = \frac{d^k}{dx^k}\phi(x)^n \qquad \text{for} \qquad k = 0, 1, \ldots, n-1$$

and

$$\phi^{(k)}(x) = \frac{d^k\phi(x)}{dx^k}$$

$$\phi^{(k)}(x_0) = \phi_0^{(k)}$$

The algorithm now becomes

$$\phi_0^{(k)} = -\frac{1}{A_1}\sum_{i=1}^{k}\frac{k!}{(k-1)!}A_{i+1}\phi_0^{(k-i)}$$

$$D_k^n = n\sum_{j=0}^{k-1}\binom{k-1}{j}D_j^{n-1}\phi_0^{(k-j)} \qquad \text{for} \qquad k = 1, 2, \ldots, n-1$$

beginning with the initial values

$$D_0^1 = \phi_0^{(0)} = \frac{1}{A_1}$$

The coefficients can now be calculated:

$$\alpha_n = \frac{1}{n!}D_{n-1}^n$$

Algebraically, the first five coefficients are

$$\alpha_1 = \frac{1}{A_1} \quad , \quad \alpha_2 = -\frac{A_2}{A_1^3}$$

$$\alpha_3 = -\frac{A_3}{A_1^4} + 2\frac{A_2^2}{A_1^5}$$

$$\alpha_4 = -\frac{A_4}{A_1^5} + 5\frac{A_2A_3}{A_1^6} - 5\frac{A_2^3}{A_1^7}$$

$$\alpha_5 = -\frac{A_5}{A_1^6} + \frac{6A_2A_4 + 3A_3^2}{A_1^7} - 21\frac{A_2^2A_3}{A_1^8} + 14\frac{A_2^4}{A_1^9} \qquad (16)$$

Each successive coefficient becomes increasingly more complex. Table 2 lists the R series coefficients for a transfer angle of 60 degrees.

TABLE 2: R Series Coefficients for $\theta = 60°$

n	α_n
1	2.876351039445733
2	-4.634718652746828
3	6.169638843024049
4	-7.677730891005001
5	9.199104623157812
6	-10.731091604324702
7	12.266169580346382
8	-13.800785808657999
9	15.334487956965681
10	-16.867784047477109
11	18.401065122700818
12	-19.934436495815678
13	21.467864111717599
14	-23.001301593856162
15	24.534730221361581
16	-26.068150929596808
17	27.601569133880563
18	-29.134987387096338
19	30.668404962779338
20	-32.201822741326474
21	33.735279494304024
22	-35.269089203411149
23	36.804909127457499
24	-38.350692931914622
25	39.939922586593518
26	-41.694275534386783

Since the recursive algorithm used to calculate the R series coefficients is slow in terms of computer time a more efficient method is desirable. The algebraic form of the coefficients were formulated into a matrix in order to determine whether a pattern existed such as for the RI series. Alternate methods of obtaining the R series coefficients examined the behavior of the coefficients as functions of n and Θ. Additionally, each series was expressed as a continued fraction so that fewer coefficients would be required in order to achieve the same accuracy as the series.

Matrix Method

Equation set (16) may be expressed in the following matrix form:

$$\begin{Bmatrix} \alpha_1 \\ \alpha_2 \\ \alpha_3 \\ \alpha_4 \\ \alpha_5 \\ . \\ \alpha_i \end{Bmatrix} = \begin{bmatrix} \frac{1}{A_1^2} & 0 & 0 & 0 & 0 & . & 0 \\ 0 & -\frac{1}{A_1^3} & 0 & 0 & 0 & . & 0 \\ 0 & \frac{2A_2}{A_1^5} & -\frac{1}{A_1^4} & 0 & 0 & . & 0 \\ 0 & -\frac{5A_2^2}{A_1^7} & \frac{5A_2}{A_1^6} & -\frac{1}{A_1^5} & 0 & . & 0 \\ 0 & \frac{14A_2^3}{A_1^9} & \frac{3A_1A_3-21A_2^2}{A_1^8} & \frac{6A_2}{A_1^7} & -\frac{1}{A_1^6} & . & 0 \\ 0 & . & . & . & . & . & 0 \\ 0 & . & . & . & . & . & -\frac{1}{A_1^{i+1}} \end{bmatrix} \begin{Bmatrix} A_1 \\ A_2 \\ A_3 \\ A_4 \\ A_5 \\ . \\ A_i \end{Bmatrix} = P\{A_n\}$$

Since the first row and the first column of P contain all zero elements, except the first element, we can look at the submatrix P':

$$P' = -\frac{1}{A_1^2}\begin{bmatrix} \frac{1}{A_1} & 0 & 0 & 0 & . & 0 \\ -\frac{2A_2}{A_1^3} & \frac{1}{A_1^2} & 0 & 0 & . & 0 \\ \frac{5A_2^2}{A_1^5} & -\frac{5A_2}{A_1^4} & \frac{1}{A_1^3} & 0 & . & 0 \\ -\frac{14A_2^3}{A_1^7} & \frac{21A_2^2-3A_1A_3}{A_1^6} & -\frac{6A_2}{A_1^5} & \frac{1}{A_1^4} & . & 0 \\ . & . & . & . & . & 0 \\ . & . & . & . & . & \frac{1}{A_1^i} \end{bmatrix} = -\frac{1}{A_1^2}R$$

The first column of the R matrix has the general form:

$$R_{i1} = \frac{(-1)^{i+1}(2i)!}{i!(i+1)!}\frac{A_2^{i-1}}{A_1^{2i-1}}$$

and the diagonal has the general form:

$$R_{ii} = \frac{1}{A_1^i}$$

For $i > 2$, the element to the left of the diagonal element has the general form:

$$R_{i,i-1} = -\frac{(i+2)A_2}{A_1^{i+1}}$$

These were the only general terms that were ascertained. Further investigation may reveal a pattern that would be beneficial in order to generate the entire matrix.

Approximating the R Series Coefficients

Two methods of approximating the R series coefficients were investigated. The first method (Method A) involved obtaining the coefficients as a function of n. The coefficients were plotted versus n for each transfer angle. A least squares analysis was then employed to fit a polynomial expressing α_n as a function of n to each curve. The second method (Method B) involved obtaining the coefficients for the R series as a function of the transfer angle. Each coefficient, α_1 through α_{16}, was plotted versus the transfer angle. Once the plots were obtained, a least squares analysis was performed to obtain a polynomial in the transfer angle for each α_n.

Continued Fraction Expansion

The final method examined involved expanding the series into a continued fraction. This method was applied to both the R series and the RI series. A continued fraction typically provides the same accuracy as the series but uses fewer coefficients. The general form of a continued fraction is

$$a_0 + \cfrac{b_1}{a_1 + \cfrac{b_2}{a_2 + \cfrac{b_3}{a_3 + \cdots}}} = \left[a_0;\ \frac{b_1}{a_1}, \frac{b_2}{a_2}, \frac{b_3}{a_3}, \ldots \right]$$

In general, the function

$$f(x) = \frac{c_{10} + c_{11}x + c_{12}x^2 + \ldots}{c_{00} + c_{01}x + c_{02}x^2 + \ldots} \qquad (17)$$

may be expanded into the continued fraction

$$f(x) = \frac{c_{10}}{c_{00} + \dfrac{c_{20}x}{c_{10} + \dfrac{c_{30}x}{c_{20} + \cdots}}} = \left[0;\ \frac{c_{10}}{c_{00}}, \frac{c_{20}x}{c_{10}}, \frac{c_{30}x}{c_{20}}, \ldots, \frac{c_{j0}x}{c_{j-1,0}}, \ldots\right] \tag{18}$$

The coefficients c_{jk} are computed recursively by the formula

$$c_{jk} = -\begin{vmatrix} c_{j-2,0} & c_{j-2,k+1} \\ c_{j-1,0} & c_{j-1,k+1} \end{vmatrix} \tag{19}$$

where $j \geq 2$.

The RI series may be written as

$$\frac{2a}{s} = \frac{B_1}{T} + f(T) \tag{20}$$

and the R series may be written as

$$\frac{s}{2a} = T f(T) \tag{21}$$

where

$$f(T) = c_{10} + c_{11}T + c_{12}T^2 + \ldots \tag{22}$$

For the RI series $c_{1k} = B_{k+2}$ and for the R series $c_{1k} = \alpha_{k+1}$ for $k = 0, 1, 2, \ldots$.

Eq (22) is of the form of Eq (17) where

$$c_{00} = 1 \quad \text{and} \quad c_{0k} = 0 \quad \text{for} \quad k = 1, 2, 3, \ldots$$

The coefficients for the continued fraction expansion may now be calculated using Eq (19). If the continued fraction is terminated so that

$$f(T) = \frac{P_k}{Q_k} = \left[0;\ \frac{c_{10}}{c_{00}}, \frac{c_{20}T}{c_{10}}, \frac{c_{30}T}{c_{20}}, \ldots, \frac{c_{k0}T}{c_{k-1,0}}\right] \tag{23}$$

then $\frac{P_k}{Q_k}$ is termed the kth convergent of the continued fraction. The convergents are found using the following formula:

$$\frac{P_k}{Q_k} = \frac{a_k P_{k-1} + b_k P_{k-2}}{a_k Q_{k-1} + b_k Q_{k-2}} \tag{24}$$

where

$$a_k = c_{k-1,0} \qquad k \geq 1$$

$$b_1 = c_{10}, \qquad b_k = c_{k0}T \qquad k > 1$$

and

$$P_0 = 0, \quad P_1 = b_1, \quad Q_0 = 1, \quad \text{and} \quad Q_1 = 1$$

Algebraically, the first four convergents are:

$$\frac{P_1}{Q_1} = c_{10} \qquad , \qquad \frac{P_2}{Q_2} = \frac{c_{10}^2}{c_{10} - c_{11}T}$$

$$\frac{P_3}{Q_3} = \frac{-c_{10}c_{11} + (c_{10}c_{12} - c_{11}^2)T}{-c_{11} + c_{12}T}$$

$$\frac{P_4}{Q_4} = \frac{(c_{10}c_{11}^2 - c_{10}^2c_{12}) + (-2c_{10}c_{11}c_{12} + c_{11}^3 + c_{10}^2c_{13})T}{(c_{11}^2 - c_{10}c_{12}) + (c_{10}c_{13} - c_{11}c_{12})T + (c_{12}^2 - c_{11}c_{13})T^2} \tag{25}$$

Equation set (25) shows the kth convergent requires up to the coefficient $c_{1,k-1}$. This means for the RI series the coefficients up to B_{k-1} are required and for the R series the coefficients up to α_k are required. The accuracy of the kth convergent was compared to the accuracy of each series using k terms.

III. Numerical Investigation

In this section all of the figures shown are for a transfer angle of 60 degrees. All other transfer angles examined were similar and representative samples are shown in the indicated appendix. To measure the accuracy, the non-dimensional time, T (defined in Eq (5)), was varied from -.95 to 1.00.

Accuracy of RI and R Series

Using the method described in the previous section, the accuracy of the RI and the R series was evaluated.

Figures 3a and 3b show plots of the Time Residual versus T for a transfer angle of 60 degrees using 5 and 15 terms of the RI series. Plots for other transfer angles are in Appendix A. Note the lack of a data point at $T = 0$. This is due to the singularity caused by the first term of the series. Five terms of the series provides good accuracy for $|T| \leq .50$ while 15 terms provides good accuracy over the interval $|T| \leq .85$. The absolute value of the maximum Time Residual for transfer angles from 30 to 360 degrees is plotted in Figures 4a - 4c for various intervals of time. As $|T| \rightarrow 1$ the maximum absolute value of the Time Residual increases for a constant number of terms. Therefore, as $|T| \rightarrow 1$ additional terms are required to maintain a specified degree of accuracy. For $|T| \leq .25$ 15 terms provides one to two orders of magnitude greater accuracy than 5 terms. For $|T| \leq .50$ 15 terms provides approximately three orders of magnitude greater accuracy than 5 terms. For $|T| \leq .85$ 15 terms provides two to three orders of magnitude greater accuracy than 5 terms up to about 240 degrees. Beyond 240 degrees there is only about one order of magnitude difference between 5 and 15 terms.

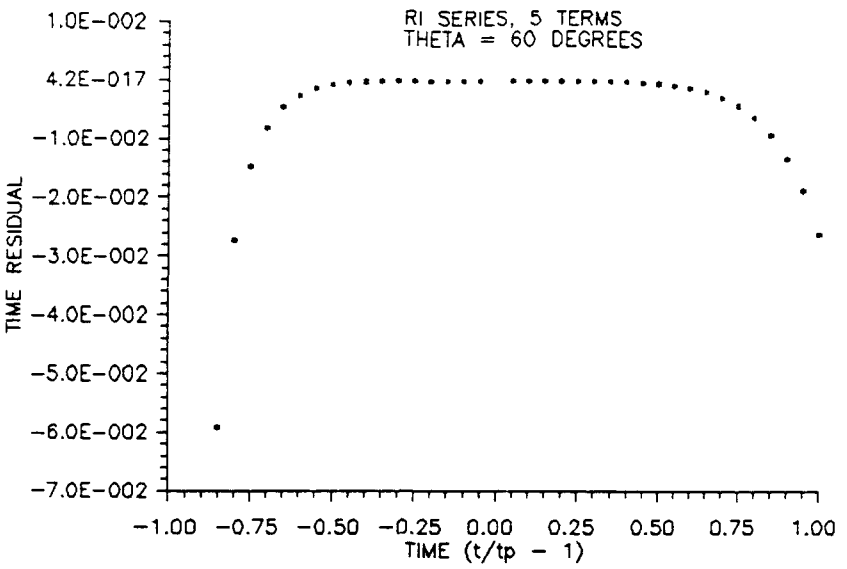

Figure 3a. Time Residual vs. T for a Transfer Angle of 60° Using 5 Terms of the RI Series

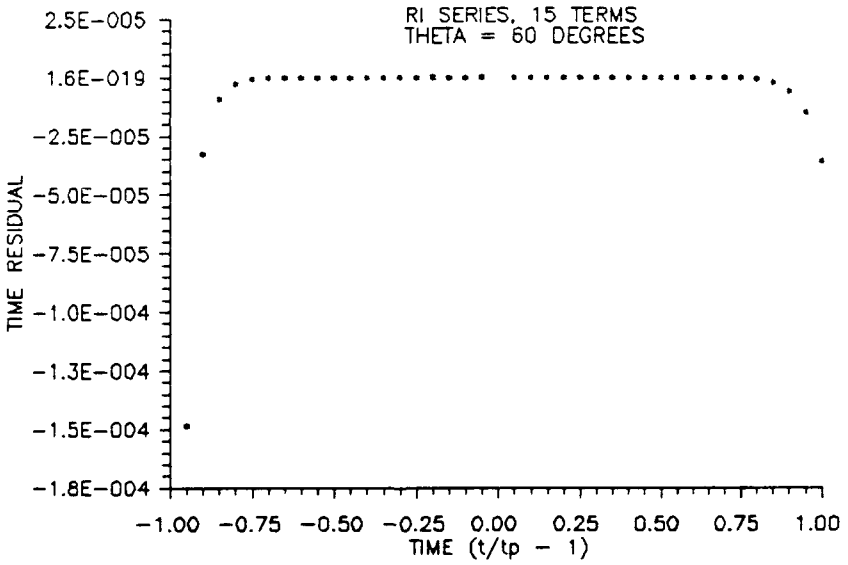

Figure 3b. Time Residual vs. T for a Transfer Angle of 60° Using 15 Terms of the RI Series

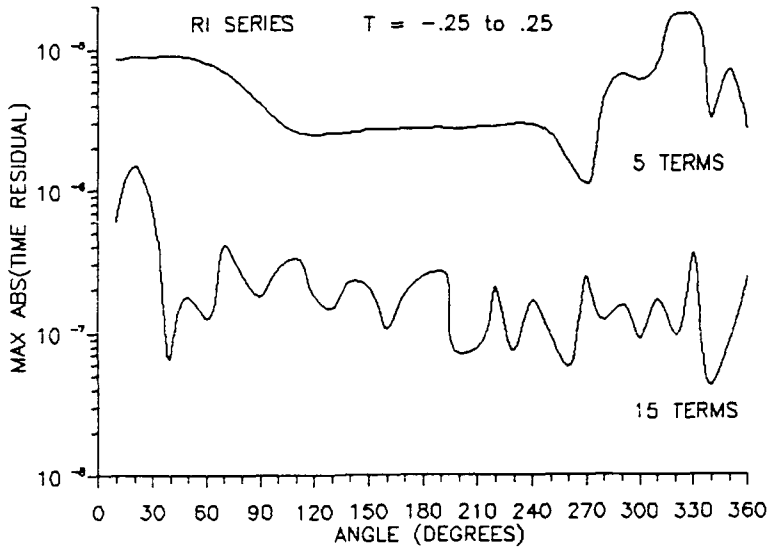

Figure 4a. Maximum Absolute Value of the Time Residual vs. Transfer Angle Using the RI Series for $T = -.25$ to $.25$

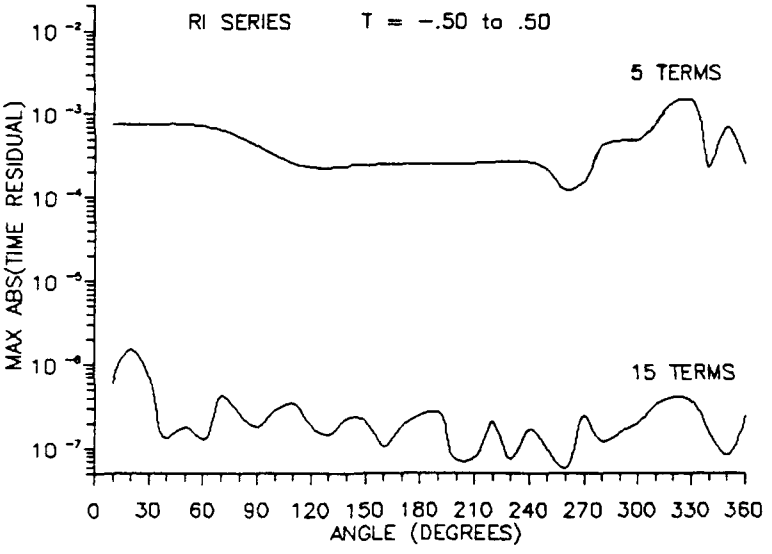

Figure 4b. Maximum Absolute Value of the Time Residual vs. Transfer Angle Using the RI Series for $T = -.50$ to $.50$

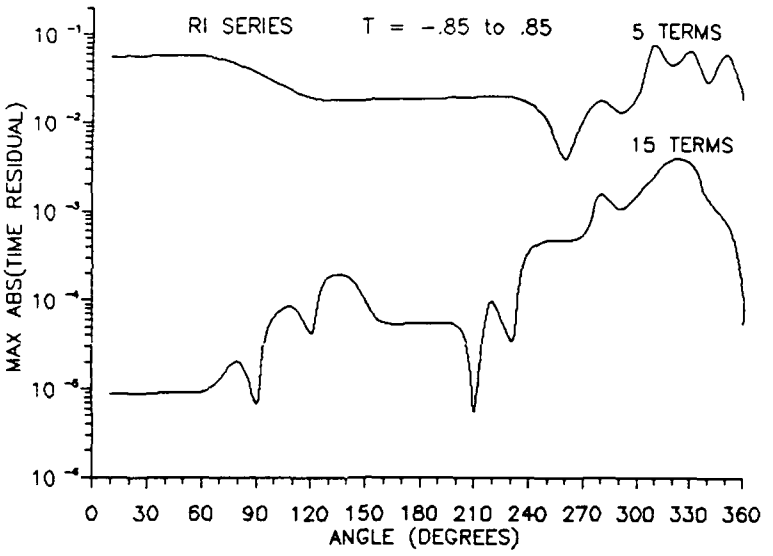

Figure 4c. Maximum Absolute Value of the Time Residual vs. Transfer Angle Using the RI Series for $T = -.85$ to $.85$

Plots of Time Residual versus T for a transfer angle of 60 degrees using 5 and 15 terms of the R series are shown in Figures 5a and 5b. Plots for other transfer angles are in Appendix B. The accuracy of the R series behaves similarly to the RI series. However, 5 terms provides good accuracy for $|T| \leq .25$ which is a much smaller interval than the RI series. Fifteen terms also provides good accuracy over a smaller interval than 15 terms of the RI series: $|T| \leq .50$. Figures 6a and 6b show plots of the absolute value of the maximum Time Residual versus transfer angle for various time intervals. For $|T| \leq .25$ 15 terms provides about four orders of magnitude greater accuracy than 5 terms. However, the R series is not as accurate as the RI series utilizing the same number of terms and has a smaller interval of convergence.

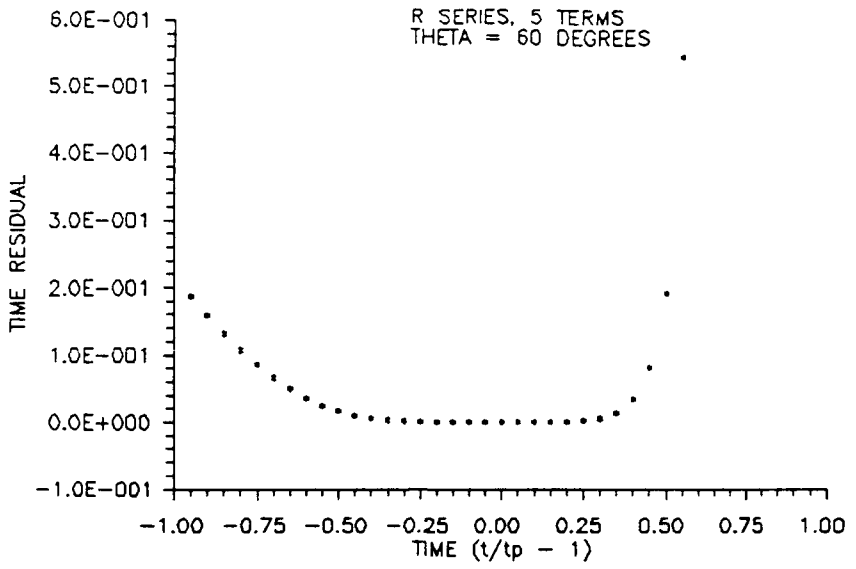

Figure 5a. Time Residual vs. T for a Transfer Angle of 60° Using 5 Terms of the R Series

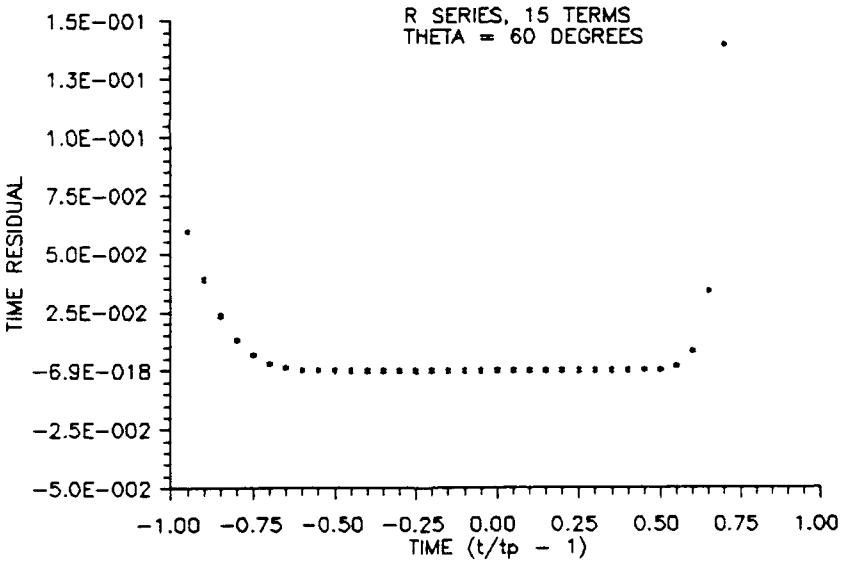

Figure 5b. Time Residual vs. T for a Transfer Angle of 60° Using 15 Terms of the R Series

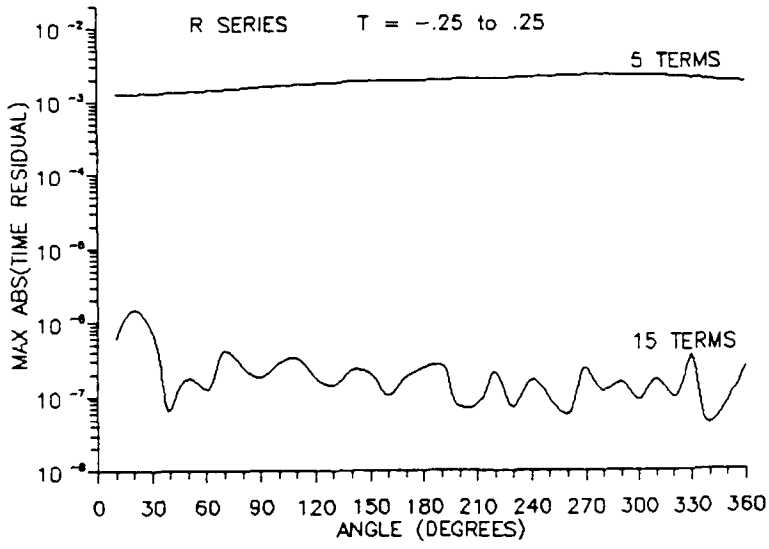

Figure 6a. Maximum Absolute Value of the Time Residual vs. Transfer Angle Using the R Series for $T = -.25$ to $.25$

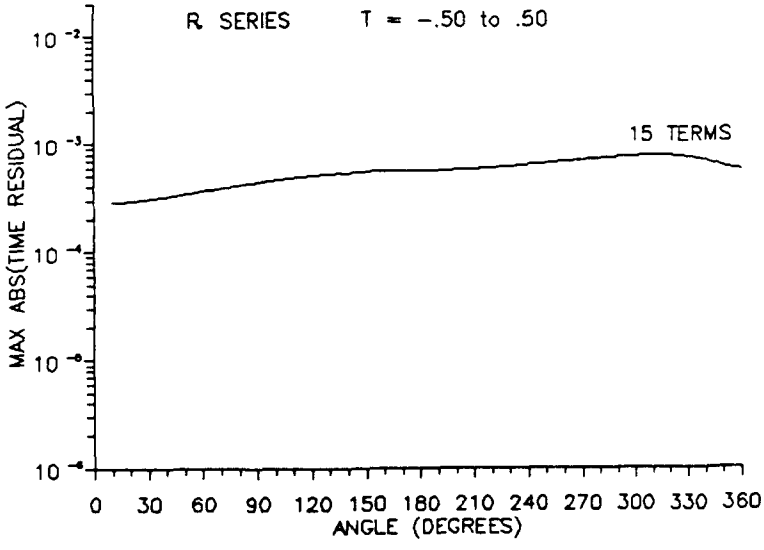

Figure 6b. Maximum Absolute Value of the Time Residual vs. Transfer Angle Using the R Series for $T = -.50$ to $.50$

Method A: R Series Coefficients as a Function of n

Figure 7 shows the absolute value of α_n is approximately a linear function of n for $n = 1$ to approximately $n = 25$. A least squares analysis was performed using 20 terms and the first 26 terms for a transfer angle of 60 degrees in order to obtain a polynomial equation. The residual shown in Figures 8a and 8b is the difference between the value of α_n calculated using the polynomial and the true value. In Figure 8a the polynomials were calculated using the first 20 terms and in Figure 8b the polynomials were calculated using the first 26 terms. Using 20 terms resulted in slightly smaller residuals. In order to reduce the residuals for the first few terms two polynomials were found. The first polynomial was for $n = 1$ to $n = m + 1$ where m is the degree of the polynomial. The second polynomial was for $n = m + 2$ to $n = 20$.

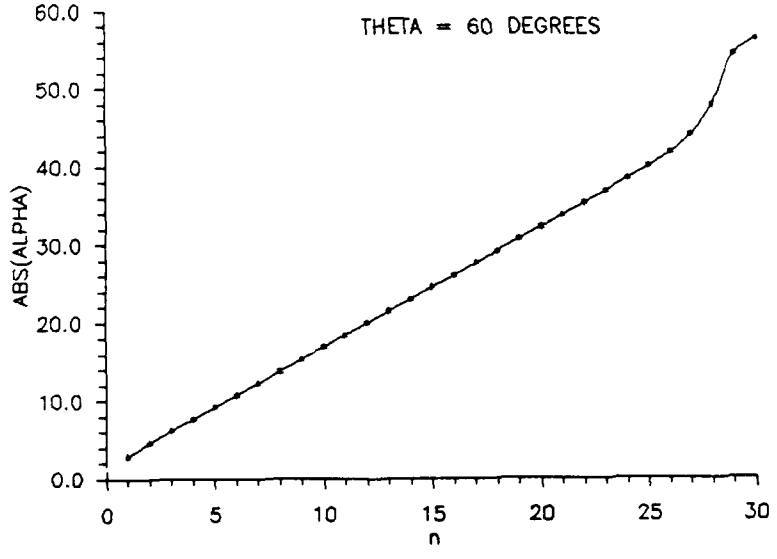

Figure 7. Absolute Value of α_n vs. n for a Transfer Angle of 60°

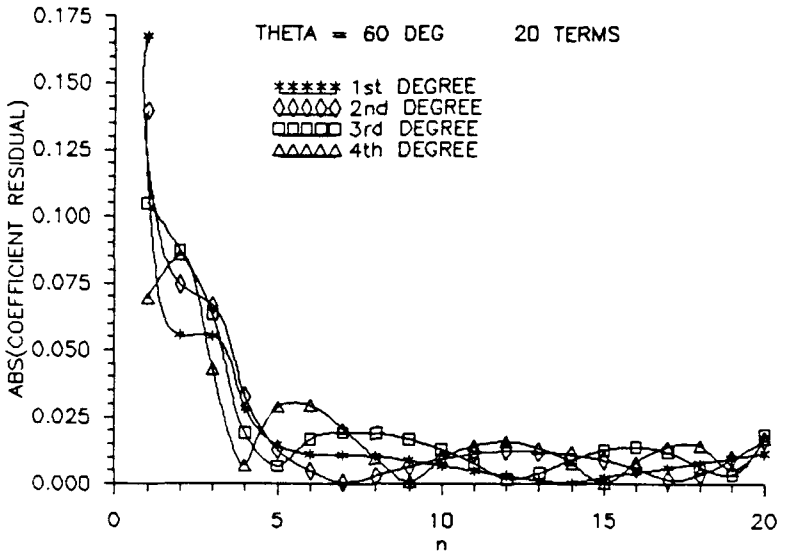

Figure 8a. Absolute Value of the Coefficient Residual vs. n for a Transfer Angle of 60° Using 20 Terms

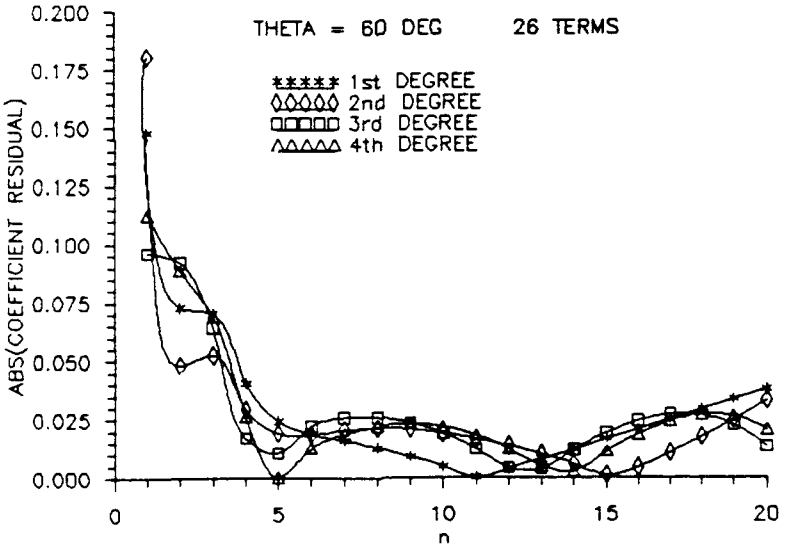

Figure 8b. Absolute Value of the Coefficient Residual vs. n for a Transfer Angle of 60° Using 26 Terms

To determine which degree of polynomial would provide the most accurate results, the absolute value of the "a Residual" (defined as the difference between the semi-major

axis calculated using the true coefficients and the value calculated using the polynomial approximation) was plotted versus T. In order to plot the absolute value of the a Residual on a logarithmic scale two plots were required: one for positive values of T and the other for negative values of T. Polynomials of degree two through degree nine were evaluated. Figures 9 - 11 show these plots using 5, 10, and 15 terms respectively.

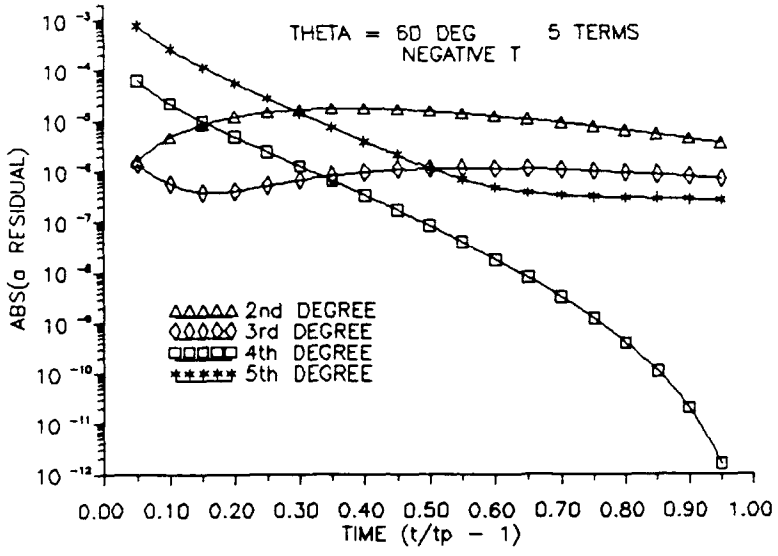

Figure 9a. Absolute Value of the a Residual vs. Negative T for a Transfer Angle of 60° Using 5 Terms with the Coefficients Calculated Using Polynomials of Degree 2 - 5

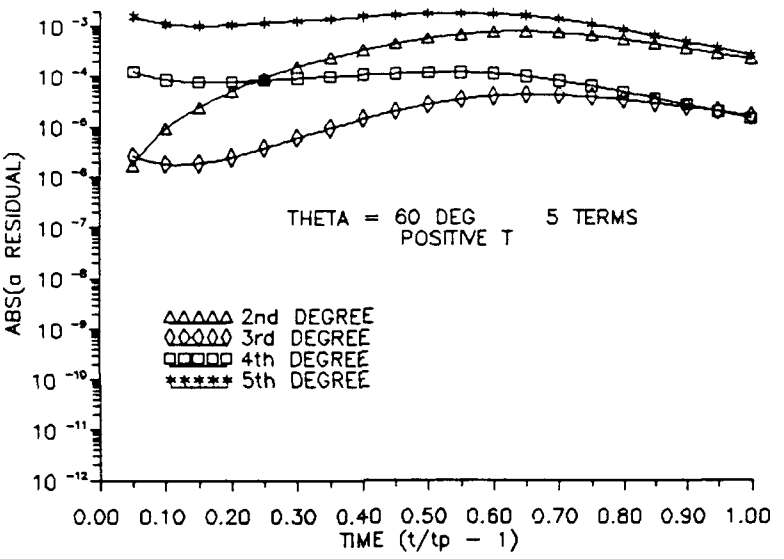

Figure 9b. Absolute Value of the a Residual vs. Positive T for a Transfer Angle of 60° Using 5 Terms with the Coefficients Calculated Using Polynomials of Degree 2 - 5

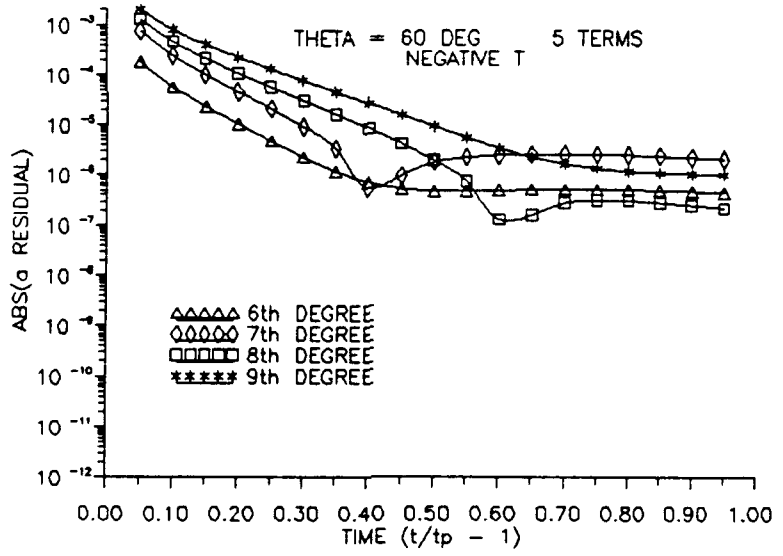

Figure 9c. Absolute Value of the a Residual vs. Negative T for a Transfer Angle of 60° Using 5 Terms with the Coefficients Calculated Using Polynomials of Degree 6 - 9

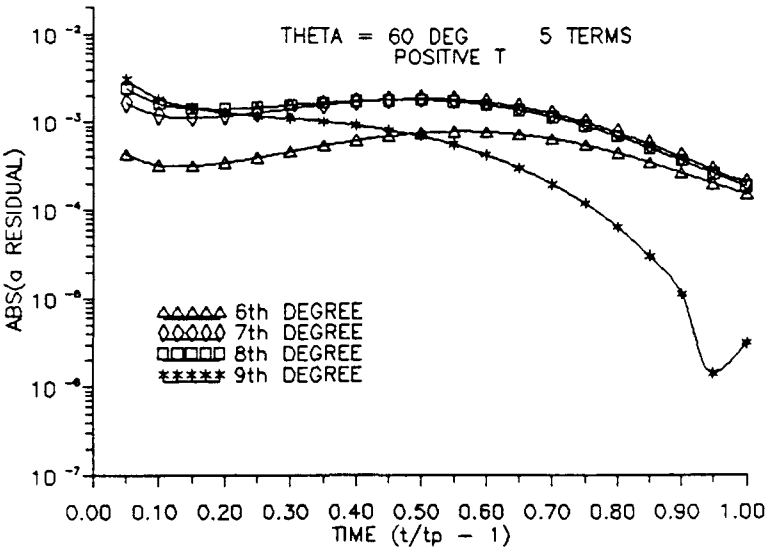

Figure 9d. Absolute Value of the a Residual vs. Positive T for a Transfer Angle of 60° Using 5 Terms with the Coefficients Calculated Using Polynomials of Degree 6 - 9

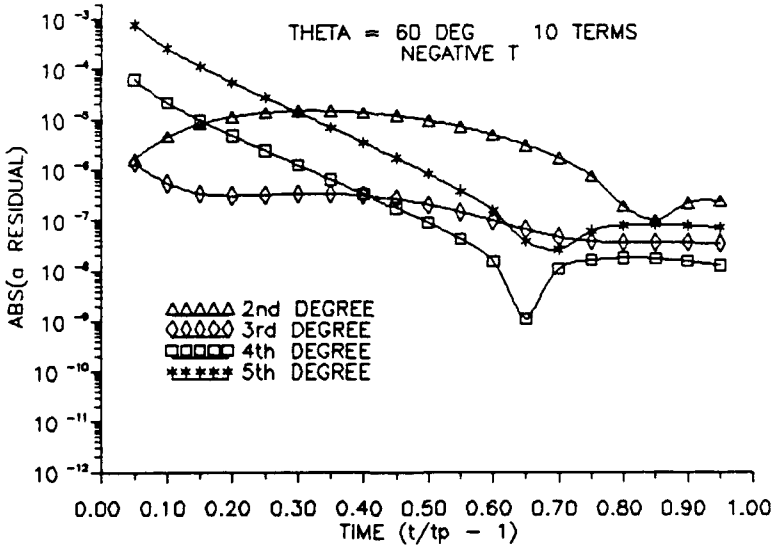

Figure 10a. Absolute Value of the a Residual vs. Negative T for a Transfer Angle of 60° Using 10 Terms with the Coefficients Calculated Using Polynomials of Degree 2 - 5

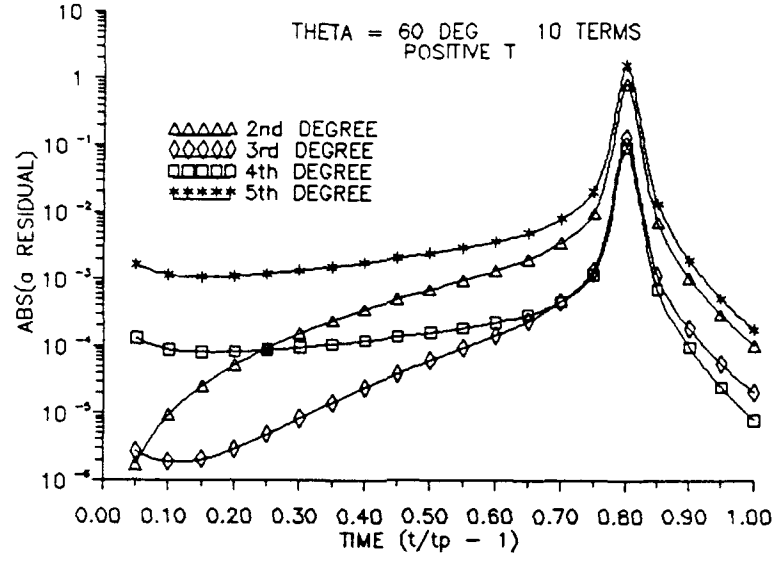

Figure 10b. Absolute Value of the a Residual vs. Positive T for a Transfer Angle of 60° Using 10 Terms with the Coefficients Calculated Using Polynomials of Degree 2 - 5

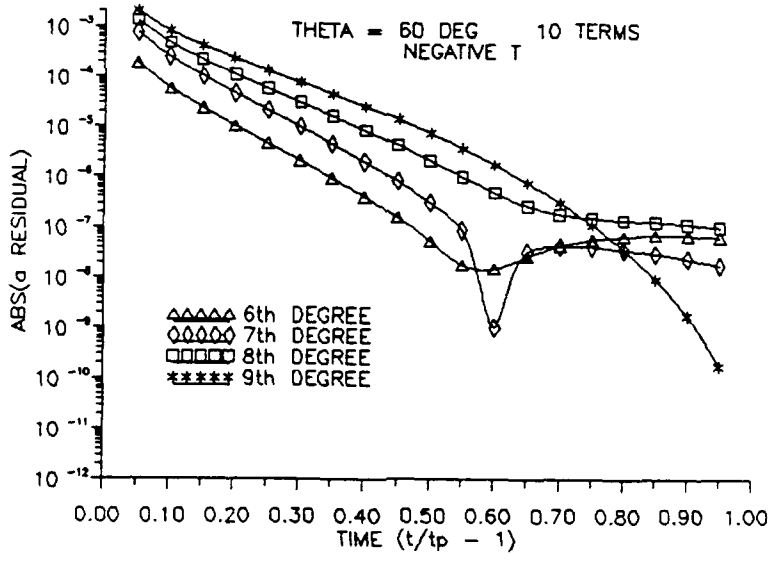

Figure 10c. Absolute Value of the a Residual vs. Negative T for a Transfer Angle of 60° Using 10 Terms with the Coefficients Calculated Using Polynomials of Degree 6 - 9

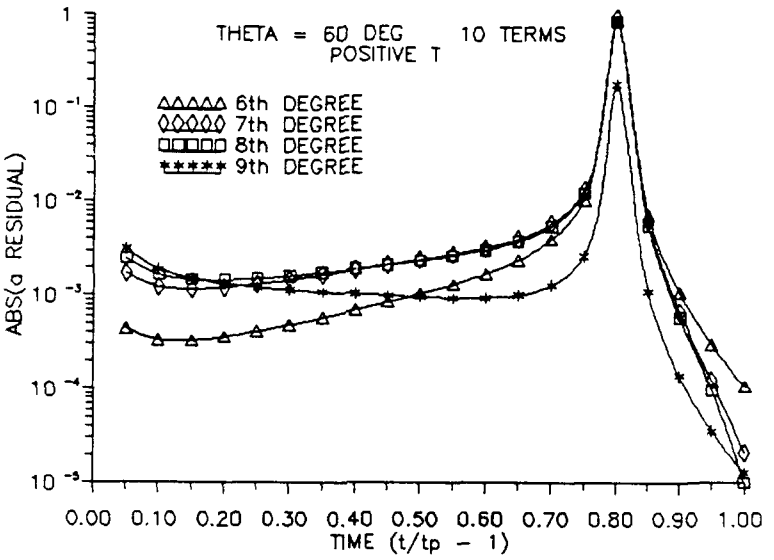

Figure 10d. Absolute Value of the a Residual vs. Positive T for a Transfer Angle of 60° Using 10 Terms with the Coefficients Calculated Using Polynomials of Degree 6 - 9

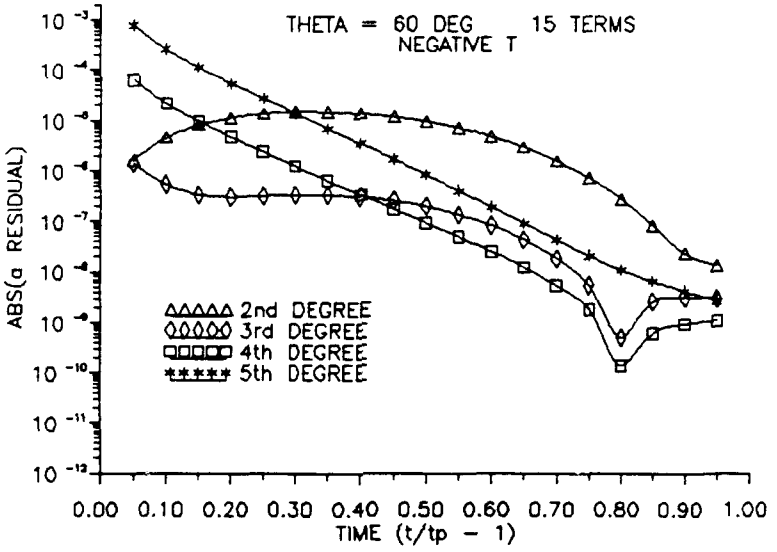

Figure 11a. Absolute Value of the a Residual vs. Negative T for a Transfer Angle of 60° Using 15 Terms with the Coefficients Calculated Using Polynomials of Degree 2 - 5

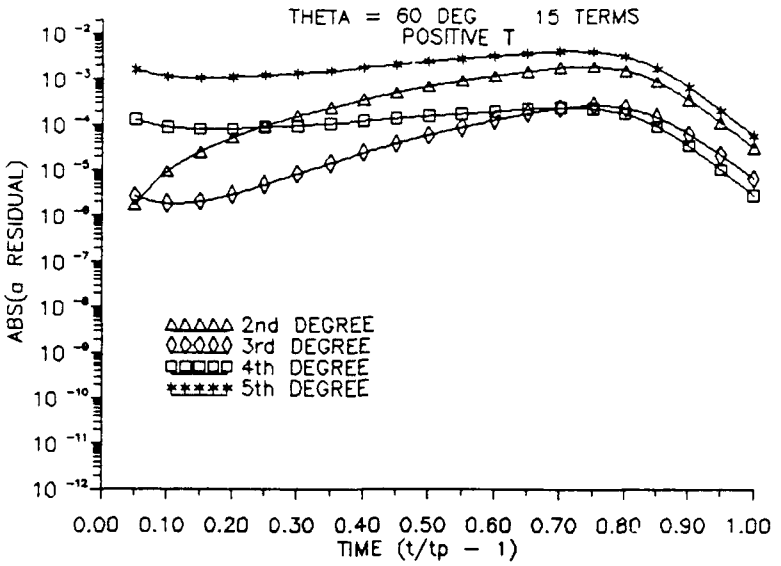

Figure 11b. Absolute Value of the a Residual vs. Positive T for a Transfer Angle of 60° Using 15 Terms with the Coefficients Calculated Using Polynomials of Degree 2 - 5

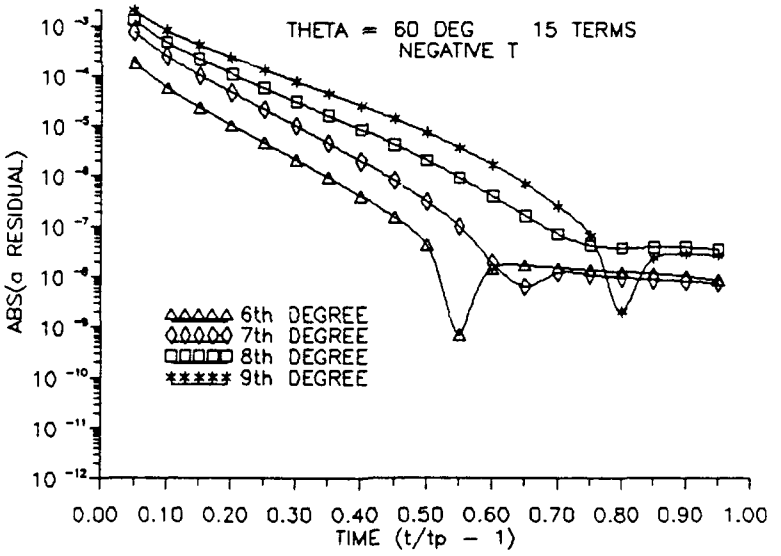

Figure 11c. Absolute Value of the a Residual vs. Negative T for a Transfer Angle of 60° Using 15 Terms with the Coefficients Calculated Using Polynomials of Degree 6 - 9

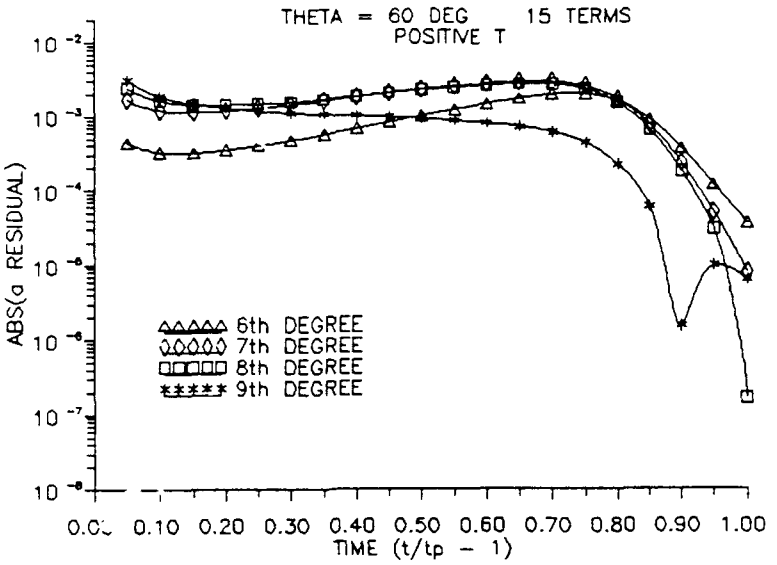

Figure 11d. Absolute Value of the a Residual vs. Positive T for a Transfer Angle of 60° Using 15 Terms with the Coefficients Calculated Using Polynomials of Degree 6 - 9

Figures 9 - 11 indicate the third degree polynomial is the most accurate approximation over the time interval $T = -.95$ to 1.00. Figures 10b and 10d show that at approximately $T = .80$ all of the polynomials give poor results using 10 terms. Checking the a Residual using 6, 8, 12, and 18 terms showed a similar spike at the same value of T. Therefore, when using this method of approximating the R series coefficients only an odd number of terms should be used.

The accuracy of this approximation using the third order polynomial was analyzed in the same manner as the true series. Figures 12a and 12b show the Time Residual versus T for a transfer angle of 60 degrees. Plots for other transfer angles are in Appendix C. The maximum absolute value of the Time Residual versus transfer angle for 5 and 15 terms is shown in Figures 13a and 13b. For $|T| \leq .25$ 15 terms provided two to four orders of magnitude greater accuracy than 5 terms. Recall that using the true coefficients resulted in a nearly constant four orders of magnitude difference.

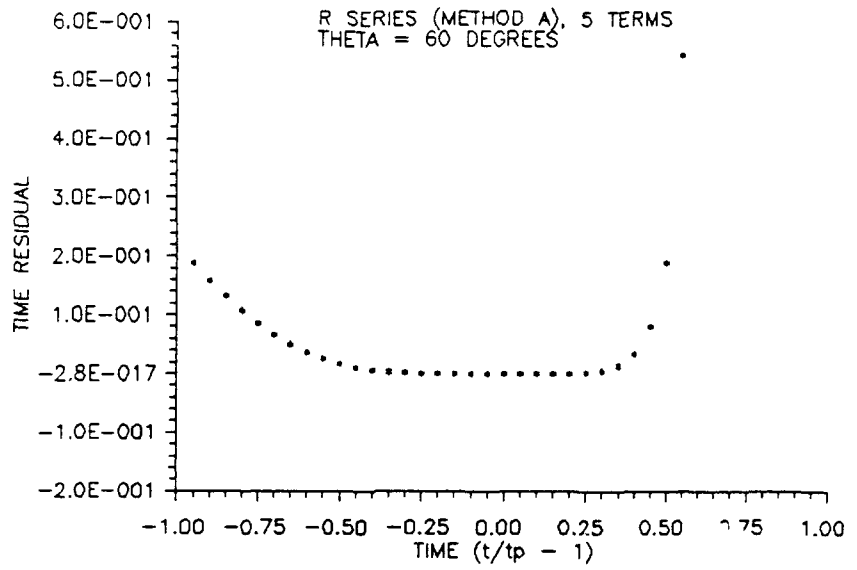

Figure 12a. Time Residual vs. T for a Transfer Angle of 60° Using 5 Terms of the R Series, Method A

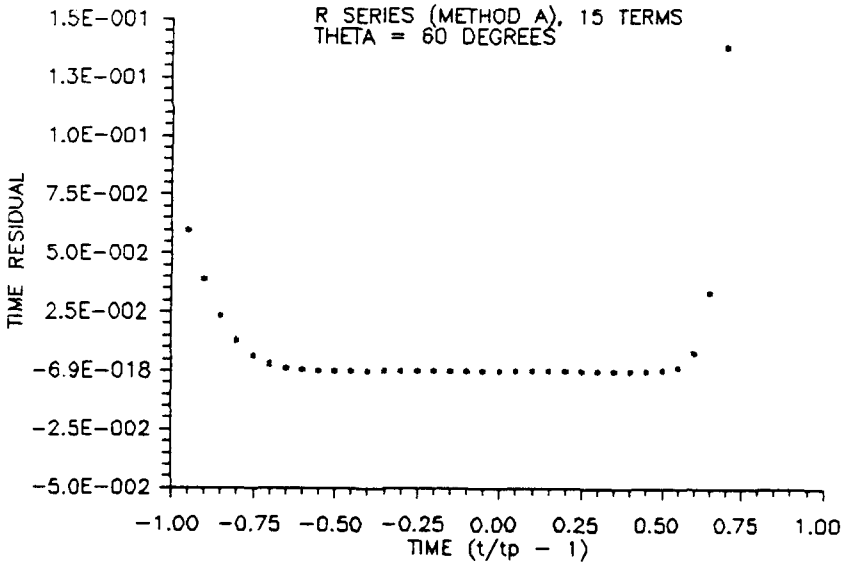

Figure 12b. Time Residual vs. T for a Transfer Angle of 60° Using 15 Terms of the R Series, Method A

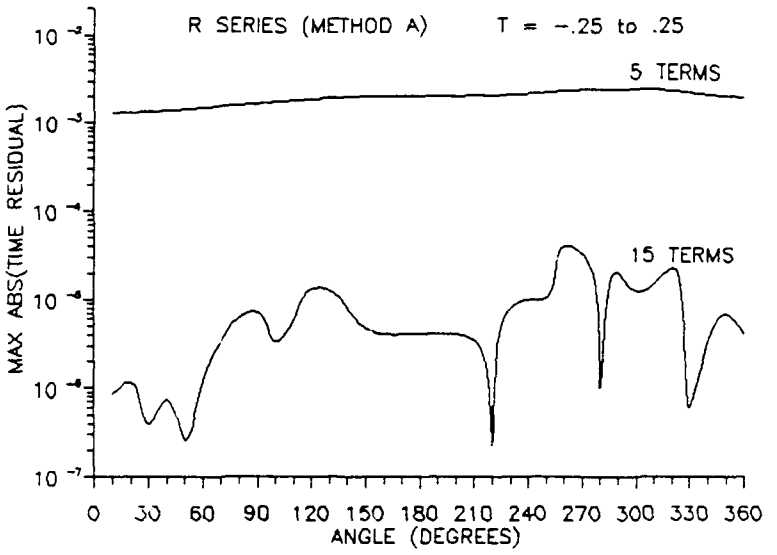

Figure 13a. Maximum Absolute Value of the Time Residual vs. Transfer Angle Using the R Series, Method A, for $T = -.25$ to $.25$

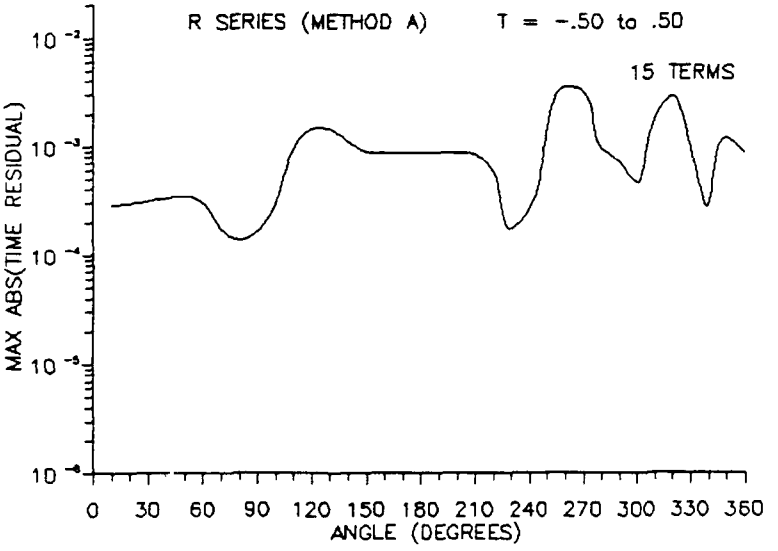

Figure 13b. Maximum Absolute Value of the Time Residual vs. Transfer Angle Using the R Series, Method A, for $T = -.50$ to $.50$

Method B: R Series Coefficients as a Function of Transfer Angle

Employing the least squares analysis an eighth order polynomial was found to best fit the plot of α_1 versus transfer angle. Therefore, an eighth order polynomial was then fit to the plots of the remaining 15 coefficients. The variance increased slightly with each successive coefficient. Figures 14a - 14d display the plots for the first four coefficients. The plots for the fifth coefficient to the sixteenth are in Appendix D. The Coefficient Residual (the absolute value of the difference between the true and the approximate coefficient) versus transfer angle is plotted in Figure 15. Each curve has nearly the same sinusoidal shape. The distance between adjacent curves decreases with each successive coefficient. See Appendix D for a plot showing Coefficient Residual for the fifth through the eighth coefficients.

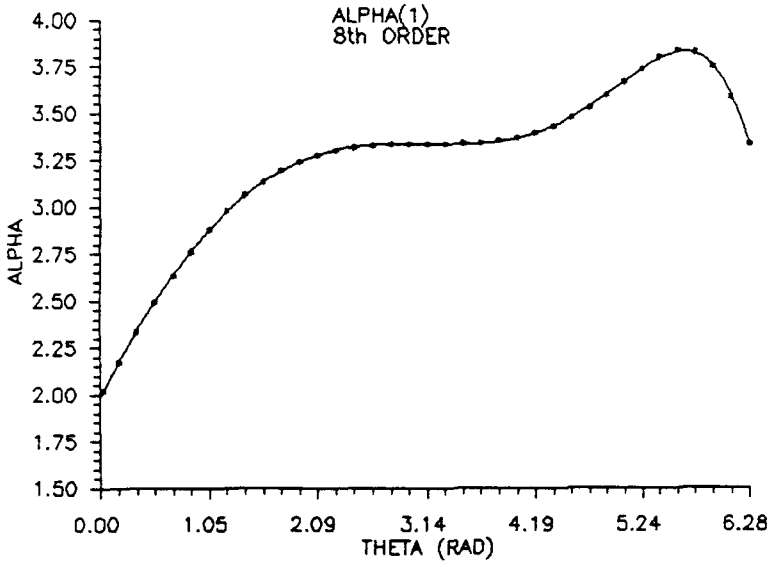

Figure 14a. α_1 vs. Transfer Angle

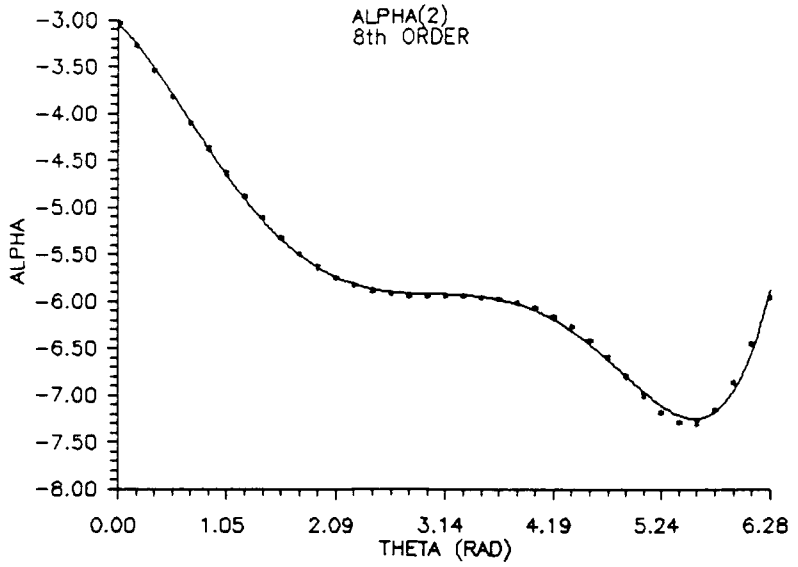

Figure 14b. α_2 vs. Transfer Angle

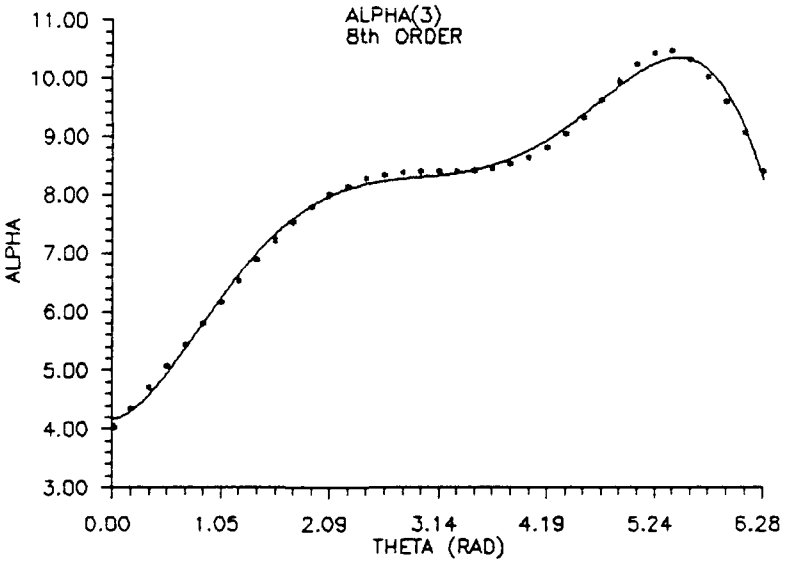

Figure 14c. α_3 vs. Transfer Angle

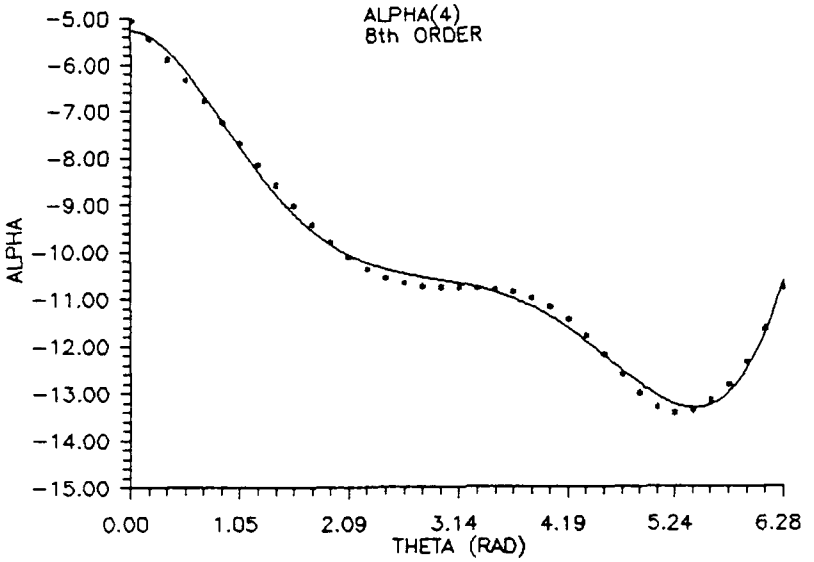

Figure 14d. α_4 vs. Transfer Angle

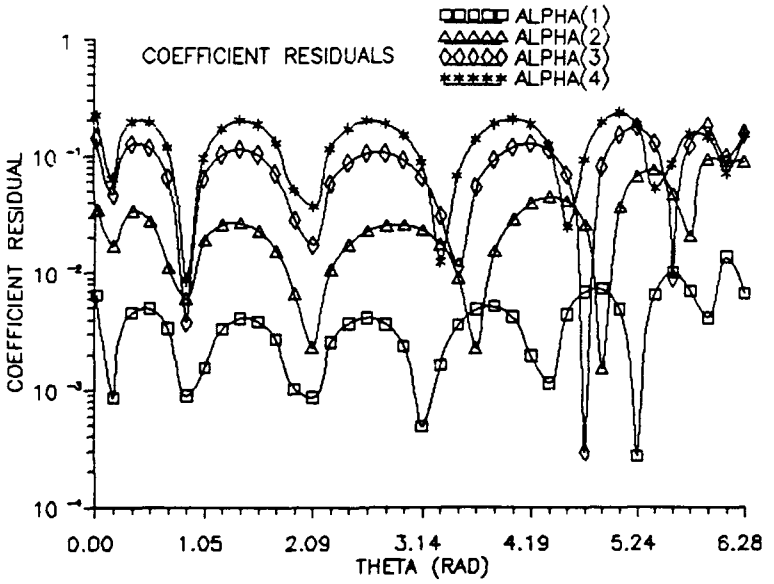

Figure 15. Coefficient Residual vs. Transfer Angle for α_1 through α_4

The accuracy of this approximation was analyzed as before. Figures 16a and 16b show the Time Residual versus T for a transfer angle of 60 degrees. Plots for other

transfer angles are in Appendix E. Figures 17a and 17b show the maximum absolute value of the Time Residual versus transfer angle for 5 and 15 terms. The difference in accuracy between 5 and 15 terms is not as great using this method as it is using the true coefficients or Method A. For some transfer angles 5 terms is more accurate than 15.

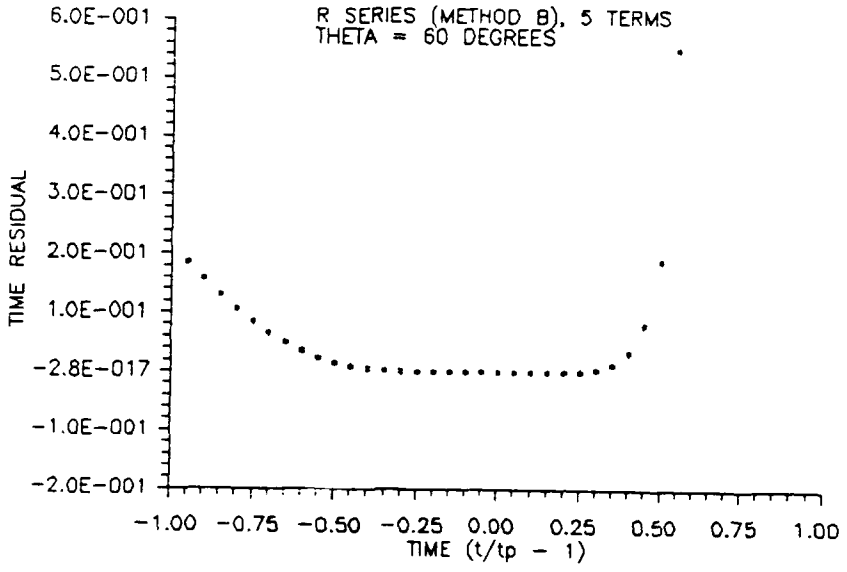

Figure 16a. Time Residual vs. T for a Transfer Angle of 60° Using 5 Terms of the R Series, Method B

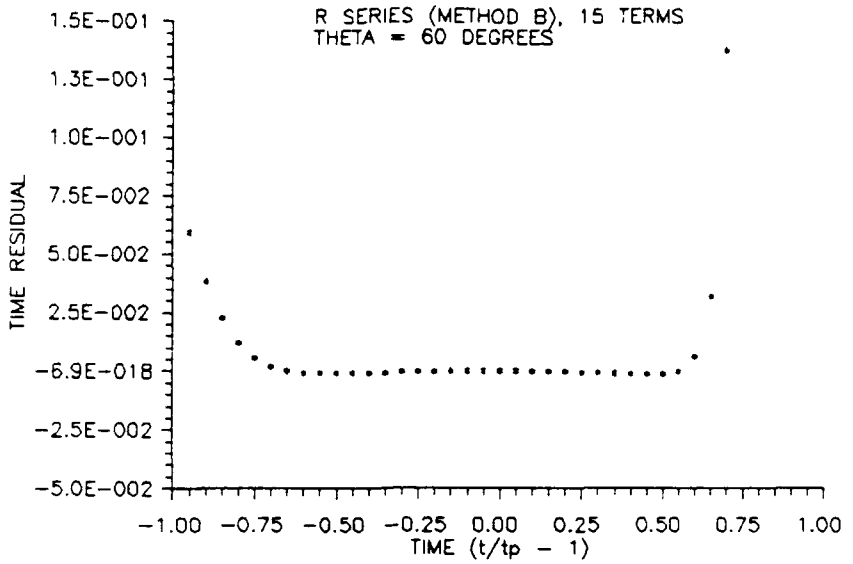

Figure 16b. Time Residual vs. T for a Transfer Angle of 60° Using 15 Terms of the R Series, Method B

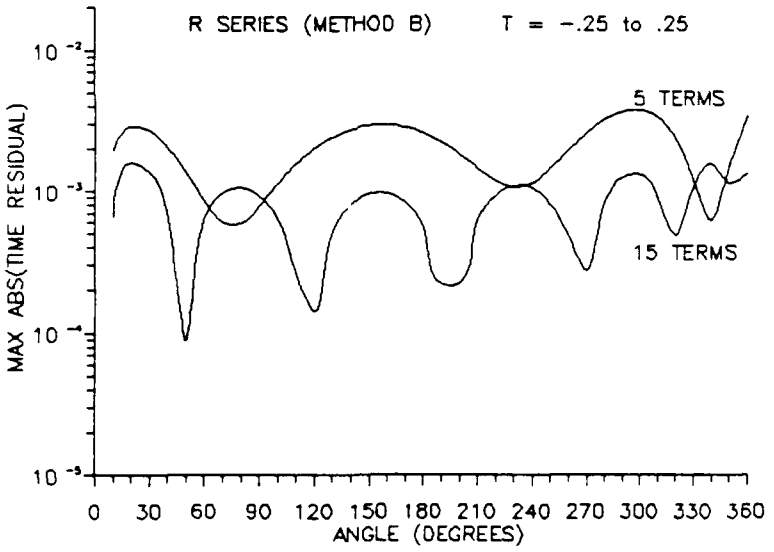

Figure 17a. Maximum Absolute Value of the Time Residual vs. Transfer Angle Using the R Series, Method B, for $T = -.25$ to $.25$

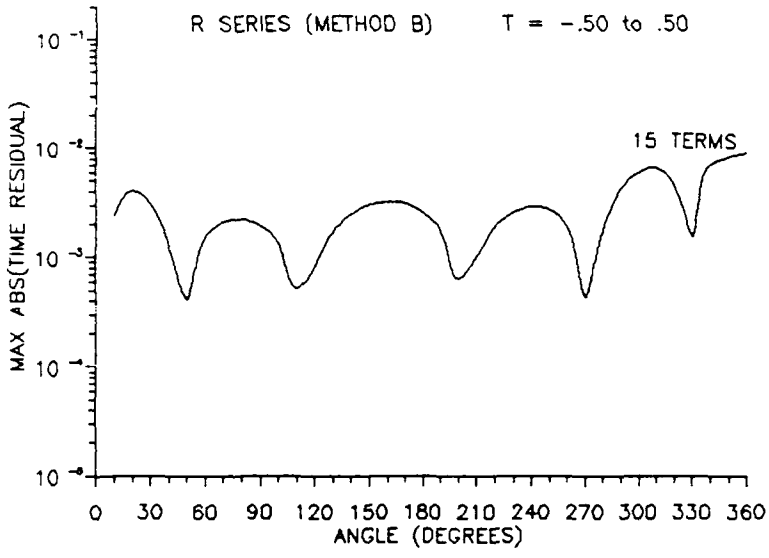

Figure 17b. Maximum Absolute Value of the Time Residual vs. Transfer Angle Using the R Series, Method B, for $T = -.50$ to $.50$

Continued Fraction Expansions

In the continued fraction expansion of the RI series the P_k and Q_k terms quickly approached zero as k increased. The twelfth convergent was the highest that could be calculated before a singularity was reached. The P_k and Q_k terms for the R series quickly increased as k increased. The highest convergent that could be calculated was the eighteenth. Therefore, the fifth and tenth convergents were selected to compare with the series using 5 and 15 terms for consistency.

Figures 18a and 18b show the plot of the Time Residual versus T for a transfer angle of 60 degrees using the continued fraction expansion of the RI series. Plots for other transfer angles are in Appendix F. The accuracy is much better for long elliptical transfers (positive T) than the RI series itself. Figures 19a - 19c show the maximum absolute value of the Time Residual versus transfer angle for the fifth and tenth convergents. Up to about 250 degrees there is very little difference between the accuracy of the fifth and tenth convergents for $|T| \leq .25$. However, for transfer angles greater than

250 degrees the tenth convergent is one to two orders of magnitude better. For $|T| \leq .50$ and $|T| \leq .85$ the tenth convergent is more accurate than the fifth. However, for some transfer angles the difference is very small especially over the interval $|T| \leq .85$.

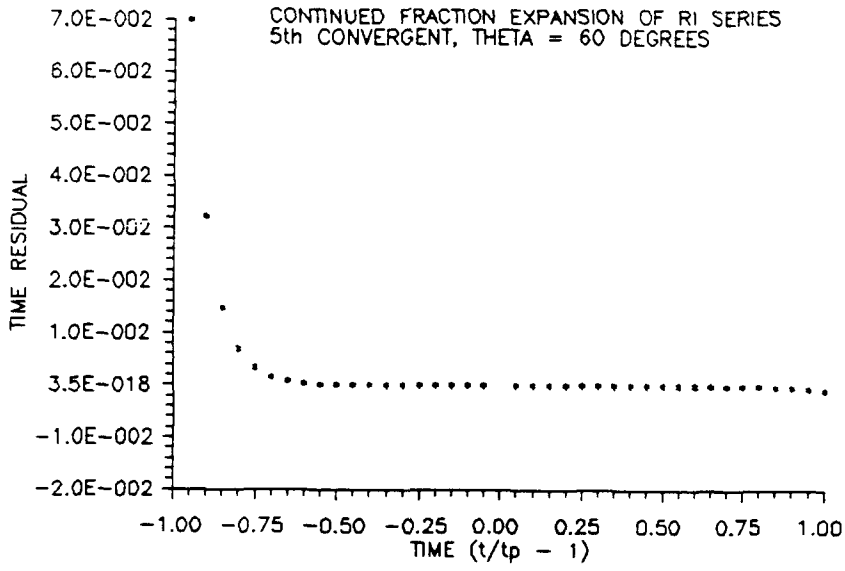

Figure 18a. Time Residual vs. T for a Transfer Angle of 60° Using the 5th Convergent of the C. F. Expansion of the RI Series

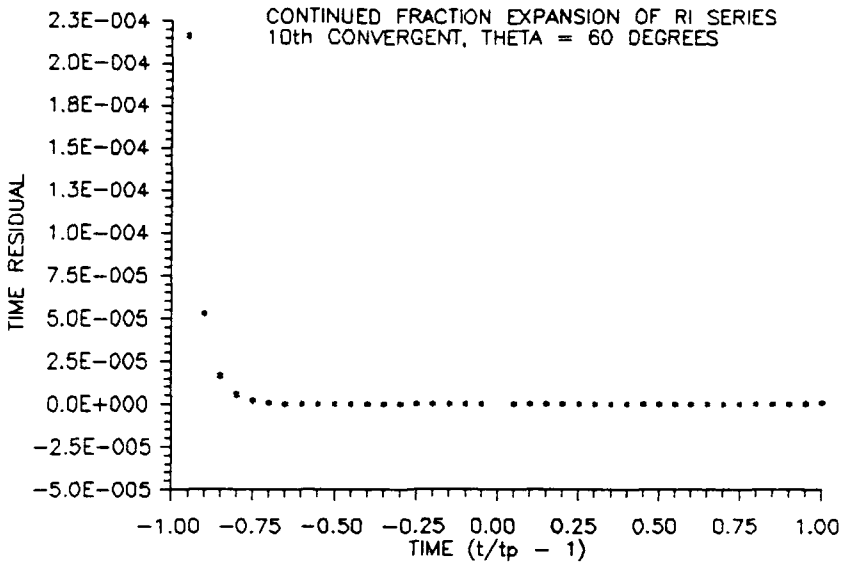

Figure 18b. Time Residual vs. T for a Transfer Angle of 60° Using the 10th Convergent of the C. F. Expansion of the RI Series

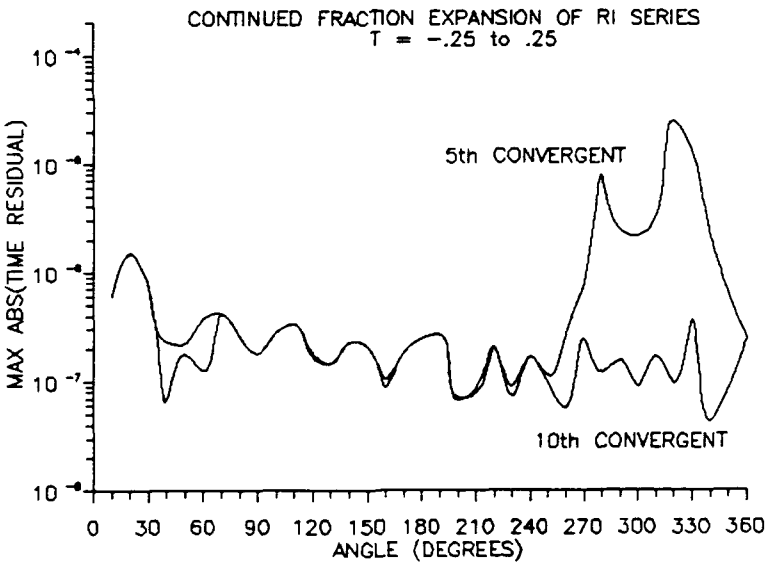

Figure 19a. Maximum Absolute Value of the Time Residual vs. Transfer Angle Using the C. F. Expansion of the RI Series for $T = -.25$ to $.25$

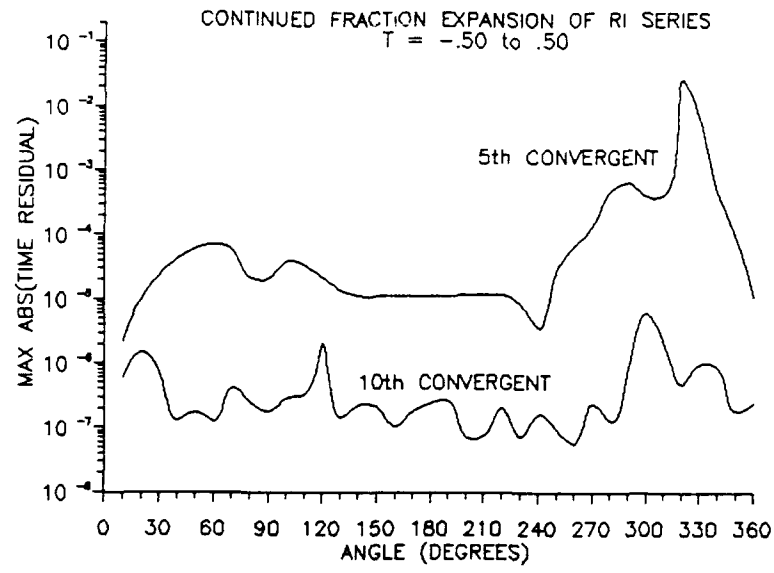

Figure 19b. Maximum Absolute Value of the Time Residual vs. Transfer Angle Using the C. F. Expansion of the RI Series for $T = -.50$ to $.50$

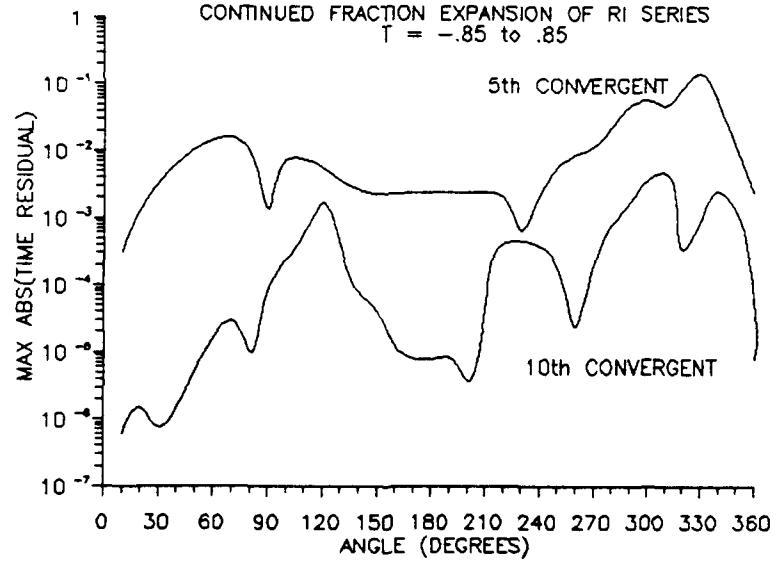

Figure 19c. Maximum Absolute Value of the Time Residual vs. Transfer Angle Using the C. F. Expansion of the RI Series for $T = -.85$ to $.85$

Figures 20a and 20b show the plots of the Time Residual versus T for a transfer angle of 60 degrees using the fifth and tenth convergents of the continued fraction expansion of the R series. Plots for other transfer angles are in Appendix G. The tenth convergent provides good accuracy for long elliptical transfers while the accuracy of the fifth convergent begins to fall off at approximately $T = .6$. Figures 21a - 21c show the maximum absolute value of the Time Residual versus transfer angle for the fifth and tenth convergents. For $|T| \leq .25$ and $|T| \leq .50$ the tenth convergent provides one to two orders of magnitude greater accuracy in most cases. However, for transfer angles less than or equal to 30 degrees there is very little difference over the interval $|T| \leq .25$. For $|T| \leq .85$ the accuracy of the tenth convergent is two to three orders of magnitude better for transfer angles less than 90 degrees. At about 230 degrees the fifth convergent is actually more accurate than the tenth.

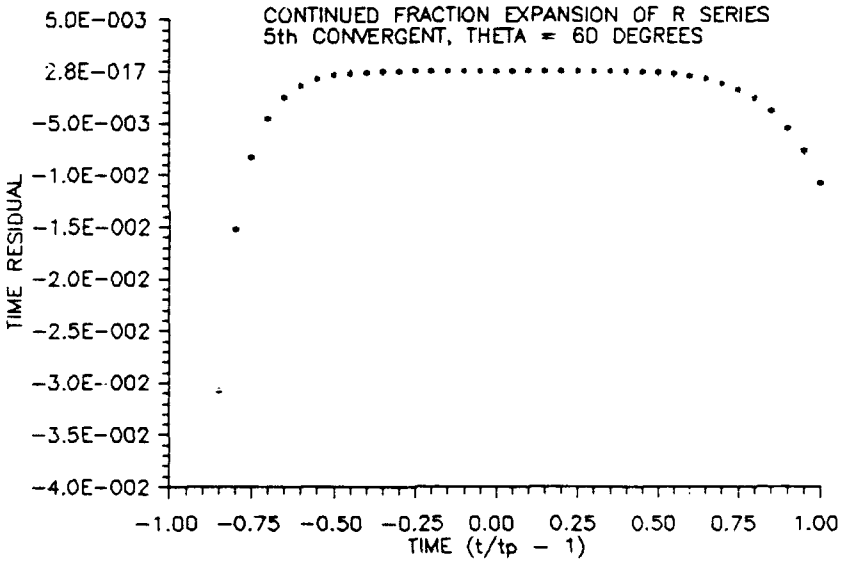

Figure 20a. Time Residual vs. T for a Transfer Angle of 60° Using the 5th Convergent of the C. F. Expansion of the R Series

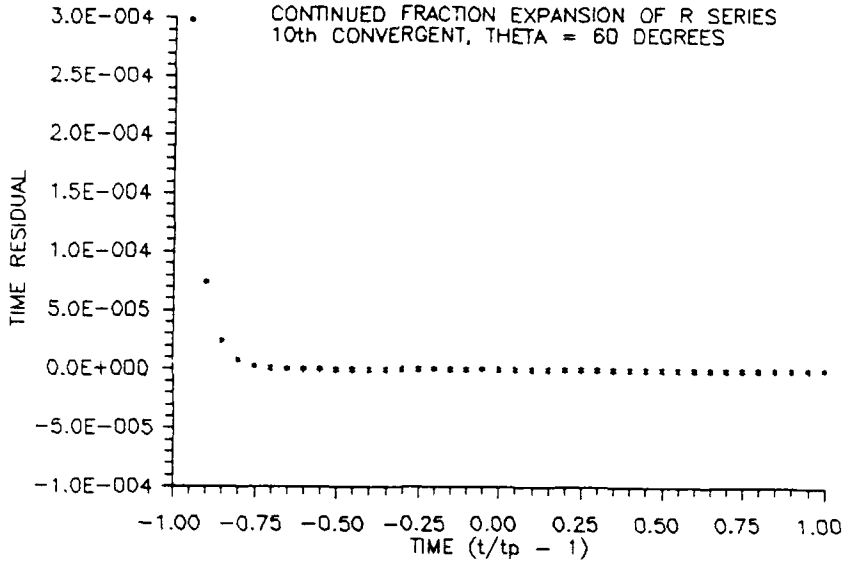

Figure 20b. Time Residual vs. T for a Transfer Angle of 60° Using the 10th Convergent of the C. F. Expansion of the R Series

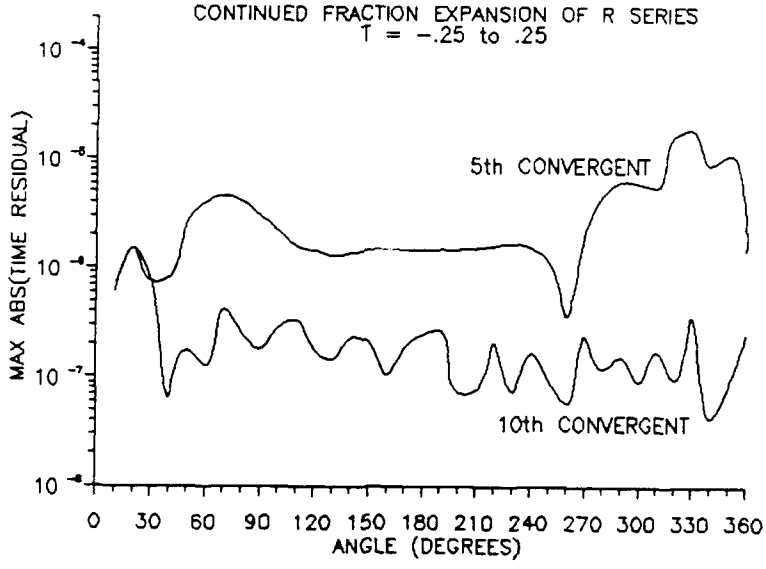

Figure 21a. Maximum Absolute Value of the Time Residual vs. Transfer Angle Using the C. F. Expansion of the R Series for $T = -.25$ to $.25$

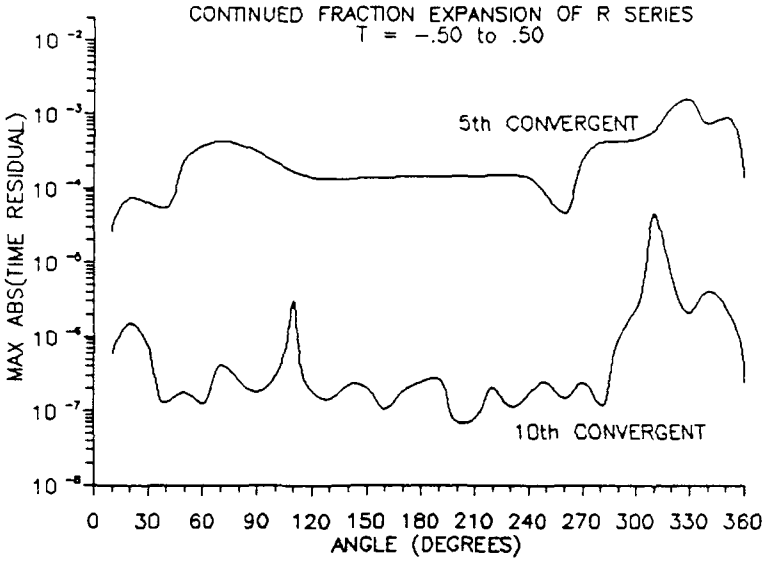

Figure 21b. Maximum Absolute Value of the Time Residual vs. Transfer Angle Using the C. F. Expansion of the R Series for $T = -.50$ to $.50$

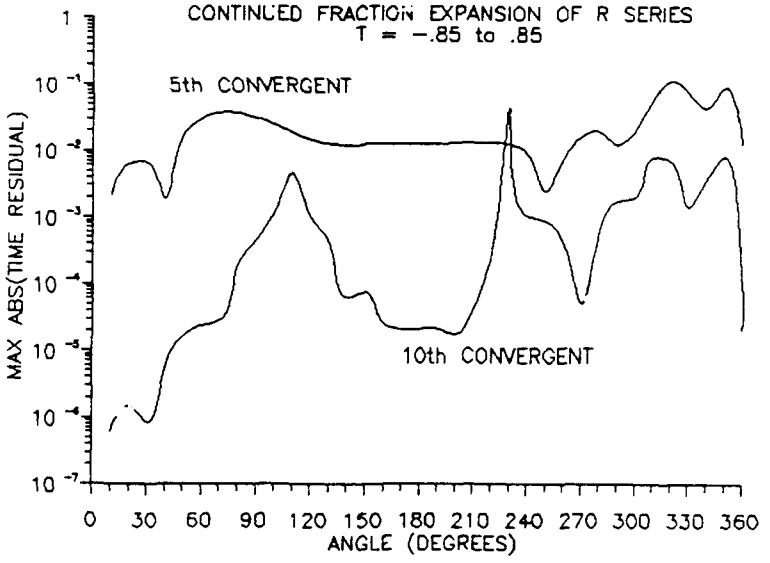

Figure 21c. Maximum Absolute Value of the Time Residual vs. Transfer Angle Using the C. F. Expansion of the R Series for $T = -.85$ to $.85$

Comparison of Methods

The RI series is more accurate than the R series by two to three orders of magnitude when using the same number of terms as shown by the plots in Figures 22a and 22b. The R series requires many more terms be used in order to obtain the same accuracy as the RI series.

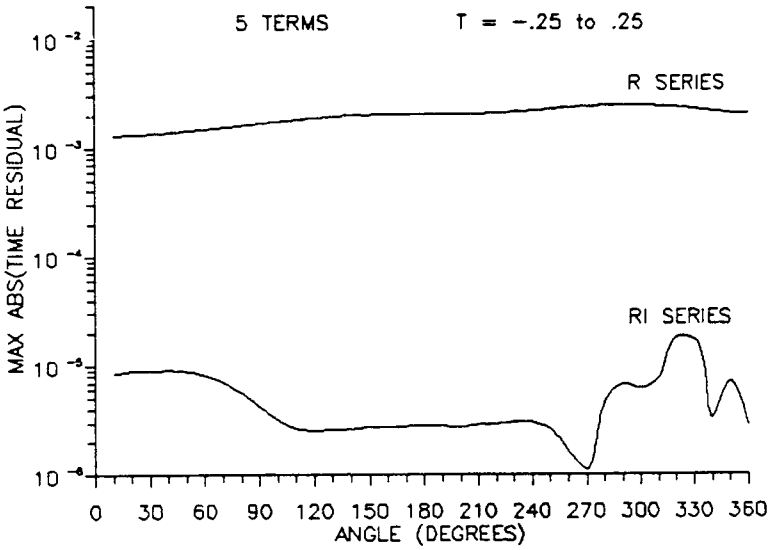

Figure 22a. Maximum Absolute Value of the Time Residual vs. Transfer Angle Using 5 Terms of the R Series and the RI Series for $T = -.25$ to $.25$

Using the alternate methods to calculate the R series coefficients did not introduce a large amount of error when 5 terms were used. The accuracy of Method A was nearly identical to the accuracy when the true coefficients were used. This is shown in Figure 23a. The accuracy of the alternate methods deteriorated when more terms of the series were used as shown in Figure 23b.

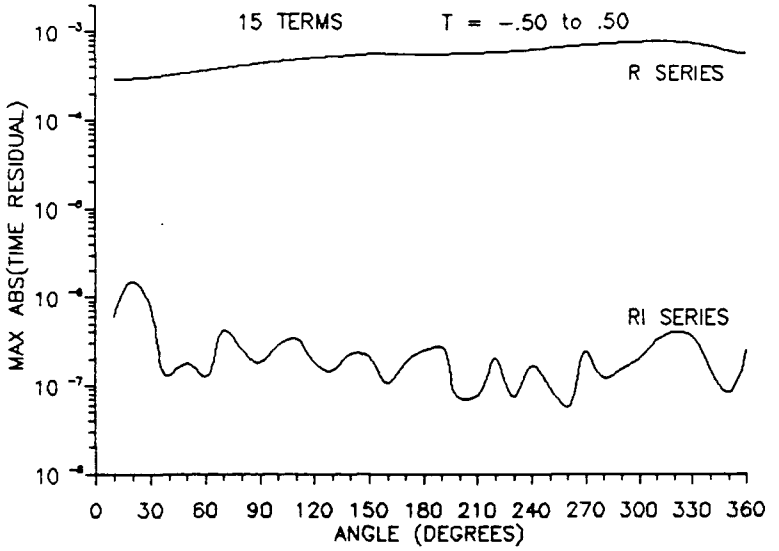

Figure 22b. Maximum Absolute Value of the Time Residual vs. Transfer Angle Using 15 Terms of the R Series and the RI Series for $T = -.50$ to $.50$

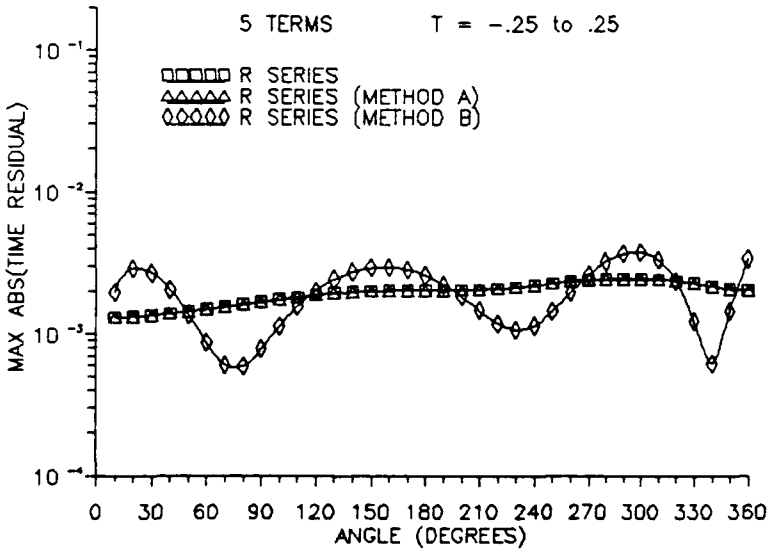

Figure 23a. Maximum Absolute Value of the Time Residual vs. Transfer Angle Using 5 Terms of the R Series With the True Coefficients, Method A, and Method B for $T = -.25$ to $.25$

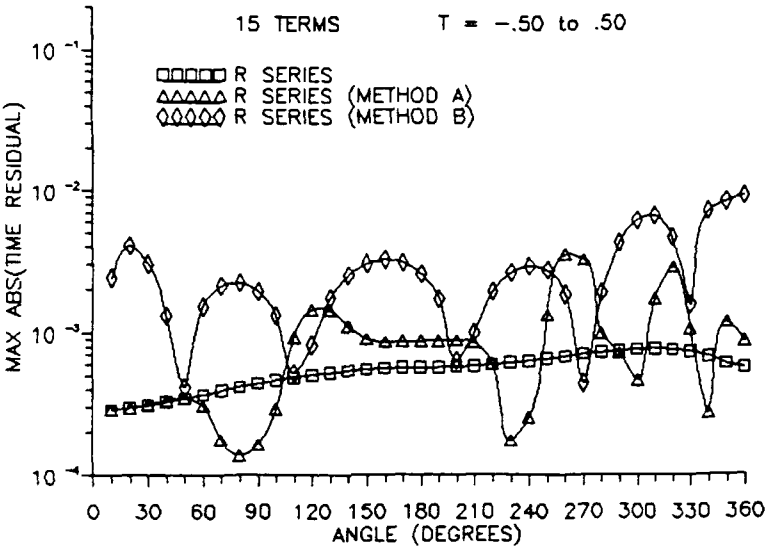

Figure 23b. Maximum Absolute Value of the Time Residual vs. Transfer Angle Using 15 Terms of the R Series With the True Coefficients, Method A, and Method B for $T = -.50$ to $.50$

Figure 24a shows that the fifth convergent of the continued fraction expansion of the RI series is more accurate than using 5 terms of the series for transfer angles less than 260 degrees. From 260 to 360 degrees the accuracy of each is approximately equal. Figure 24b illustrates the efficiency of the continued fraction expansion. The tenth convergent requires eleven coefficients and provides nearly the same accuracy as 15 terms of the RI series.

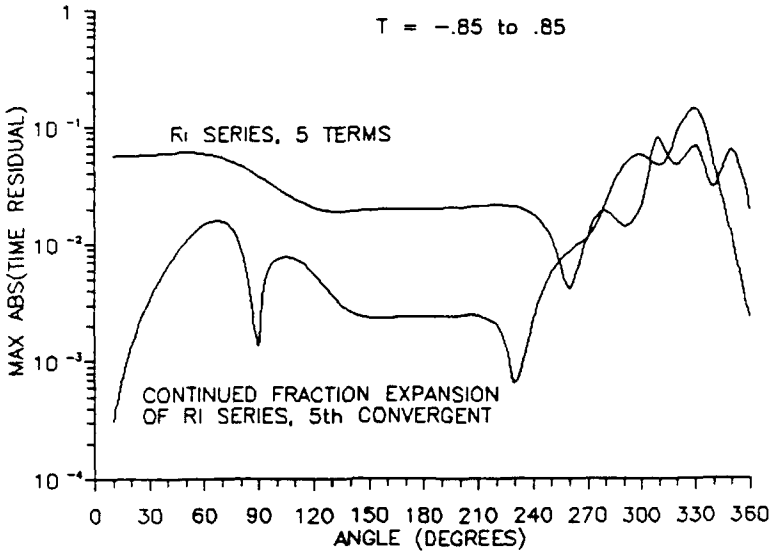

Figure 24a. Maximum Absolute Value of the Time Residual vs. Transfer Angle Using 5 Terms of the RI Series and the 5th Convergent of the C. F. Expansion of the RI Series for $T = -.85$ to $.85$

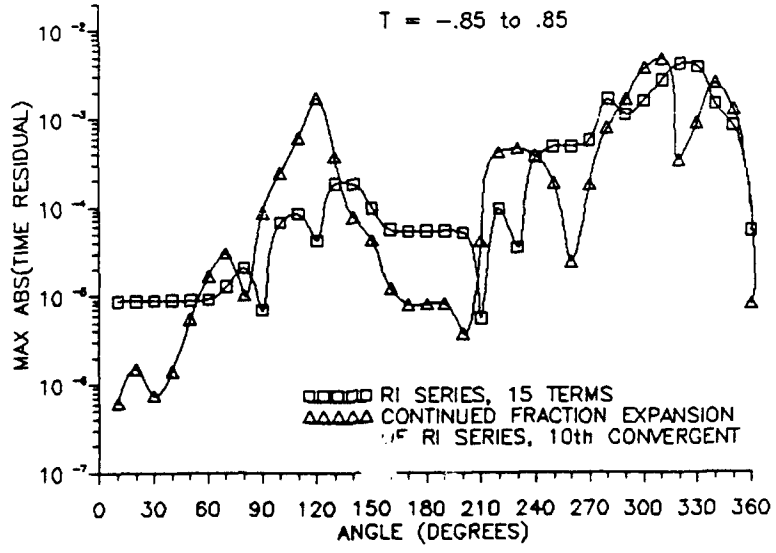

Figure 24b. Maximum Absolute Value of the Time Residual vs. Transfer Angle Using 15 Terms of the RI Series and the 10th Convergent of the C. F. Expansion of the RI Series for $T = -.85$ to $.85$

The continued fraction expansion of the R series provided approximately three orders of magnitude greater accuracy than the R series using five coefficients for each. This is shown in Figure 25a. Figure 25b indicates the continued fraction expansion still provides approximately three orders of magnitude greater accuracy with the tenth convergent compared to 15 terms of the series.

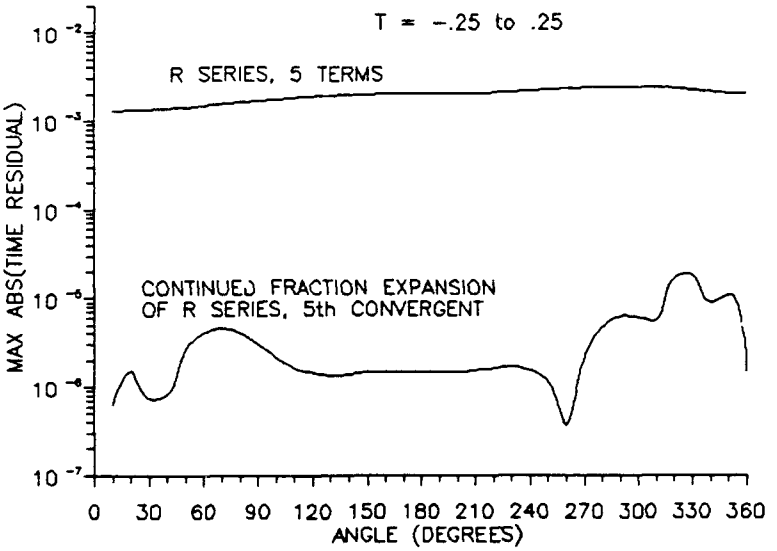

Figure 25a. Maximum Absolute Value of the Time Residual vs. Transfer Angle Using 5 Terms of the R Series and the 5th Convergent of the C. F. Expansion of the R Series for $T = -.25$ to $.25$

Using the continued fraction expansion, the R series approached the accuracy of the RI series. For the fifth convergent, the accuracy of the R series is nearly identical to the RI series for transfer angles greater than 250 degrees. Below 250 degrees the RI series is still approximately an order of magnitude more accurate. This is shown in Figures 26a and 26b for two time intervals. When the tenth convergent is used, the accuracy of the two series is nearly identical for $T = -.85$ to $.85$ and is identical for $T = -.25$ to $.25$ as shown in Figures 27a and 27b.

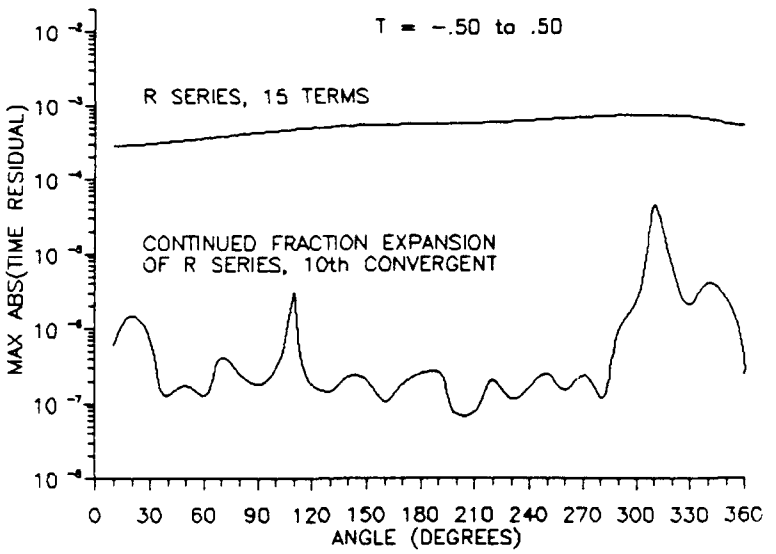

Figure 25b. Maximum Absolute Value of the Time Residual vs. Transfer Angle Using 15 Terms of the R Series and the 10th Convergent of the C. F. Expansion of the R Series for $T = -.50$ to $.50$

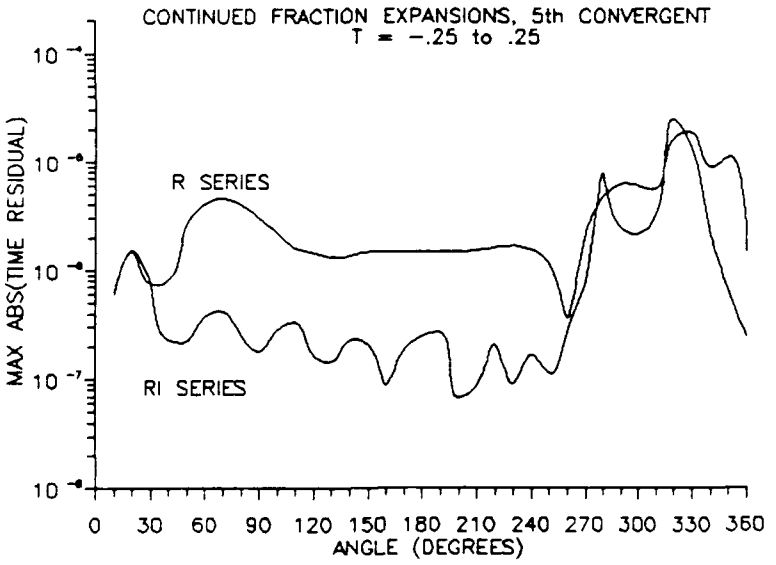

Figure 26a. Maximum Absolute Value of the Time Residual vs. Transfer Angle Using the 5th Convergent of the C. F. Expansions of the R and the RI Series for $T = -.25$ to $.25$

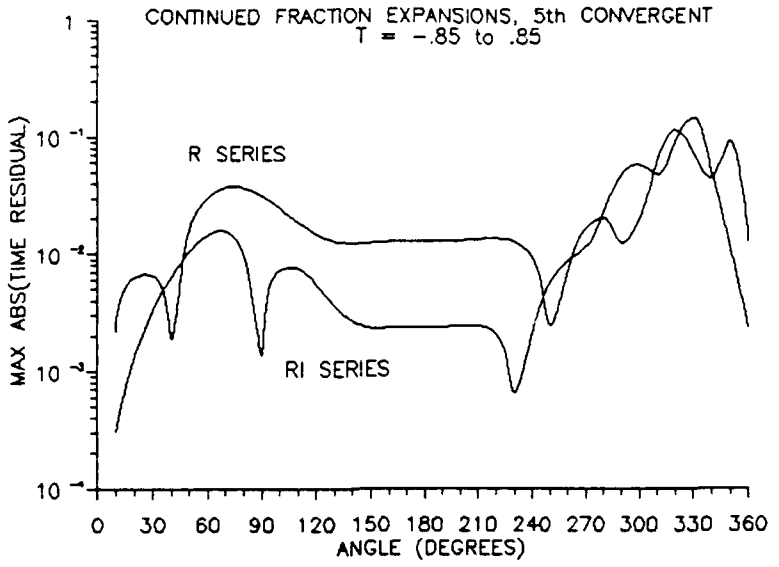

Figure 26b. Maximum Absolute Value of the Time Residual vs. Transfer Angle Using the 5th Convergent of the C. F. Expansions of the R and the RI Series for $T = -.85$ to $.85$

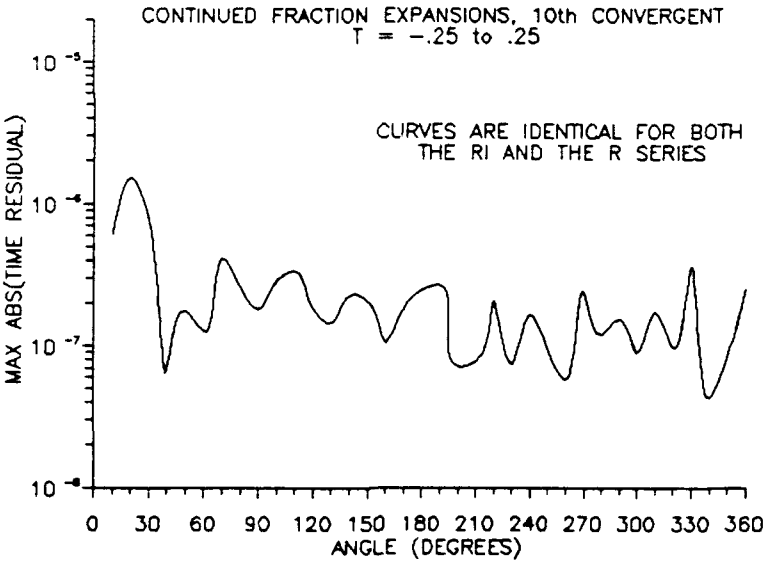

Figure 27a. Maximum Absolute Value of the Time Residual vs. Transfer Angle Using the 10th Convergent of the C. F. Expansions of the R and the RI Series for $T = -.25$ to $.25$

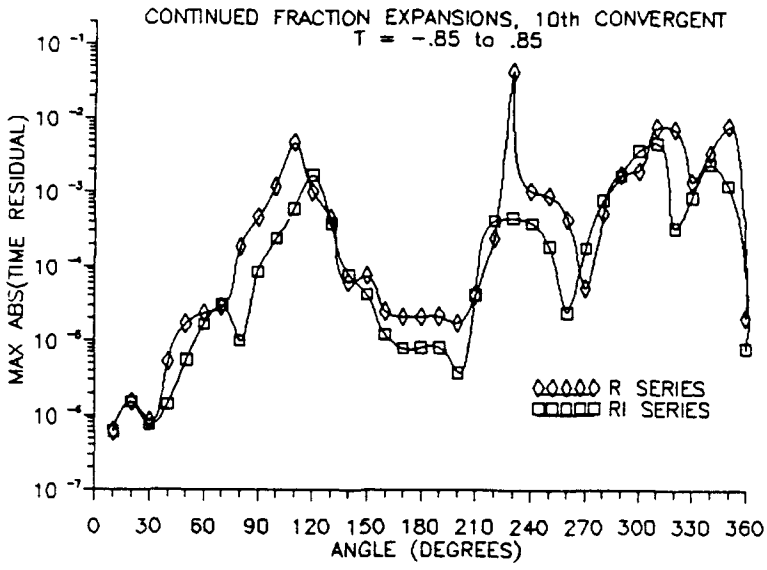

Figure 27b. Maximum Absolute Value of the Time Residual vs. Transfer Angle Using the 10th Convergent of the C. F. Expansions of the R and the RI Series for $T = -.85$ to $.85$

IV. Conclusions

Performing a series reversion on Eq (5) avoids the singularity in the RI series. However, the R series is not as accurate as the RI series with the same number of terms. Another disadvantage of the R series involves calculating the coefficients which is very computer intensive.

Alternate methods of calculating the R series coefficients using polynomial approximations were found to be nearly as accurate as the true R series coefficients. However, these methods are empirical and do not provide any advantage.

Expanding each series into a continued fraction provided the most accurate method of calculating the semi-major axis. The continued fraction expansions were most notably more accurate than each series for long elliptical transfers approaching the minimum energy transfer time. The R series continued fraction expansion was as accurate as the RI series continued fraction expansion with the benefit of no singularities. For a specified degree of accuracy the continued fraction expansion is more advantageous than the series because fewer series coefficients are required.

The accuracy of each of the methods presented was dependent upon the number of series terms or the order of the convergent, the transfer time, and especially the transfer angle. The best accuracy obtained in this study was a Time Residual on the order of 10^{-7}. For a given number of terms or convergent this varied by as much as several orders of magnitude depending upon the transfer time and transfer angle. The largest reduction in accuracy usually occurred for transfer angles between 270 and 350 degrees. As T approached the limit for which the number of terms or convergent was able to provide good results the accuracy was very sensitive to the transfer angle. For transfer times well within the limit the accuracy did not vary by more than one order of magnitude.

V. Recommendations for Further Study

During the course of this research the radius vectors were held constant while the transfer angle was varied. Further analysis of the accuracy may be accomplished while varying the radius vectors and the transfer angle. Also, further analysis of the accuracy may reveal the optimum number of terms to use.

In order to take full advantage of the R series, a more efficient method of obtaining the coefficients must be found. Further investigation of the **R** matrix may reveal a pattern that would be beneficial in order to generate the entire matrix.

While the continued fraction expansion may appear to be an attractive method of calculating the semi-major axis it has the disadvantage of being computer intensive. Therefore, it may be desirable to approximate the continued fraction using a Chebyshev polynomial.

Appendix A. *Time Residual vs. T Plots for RI Series*

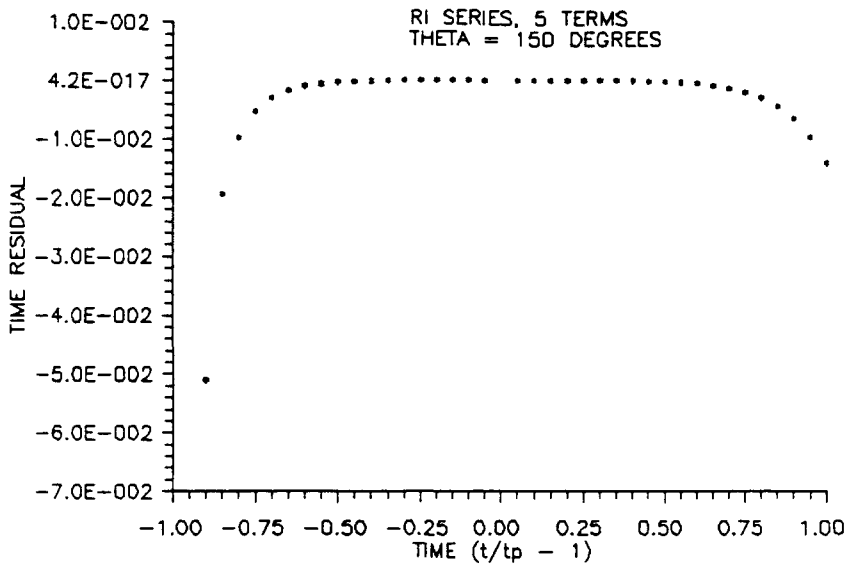

Figure 28a. Time Residual vs. T for a Transfer Angle of 150° Using 5 Terms of the RI Series

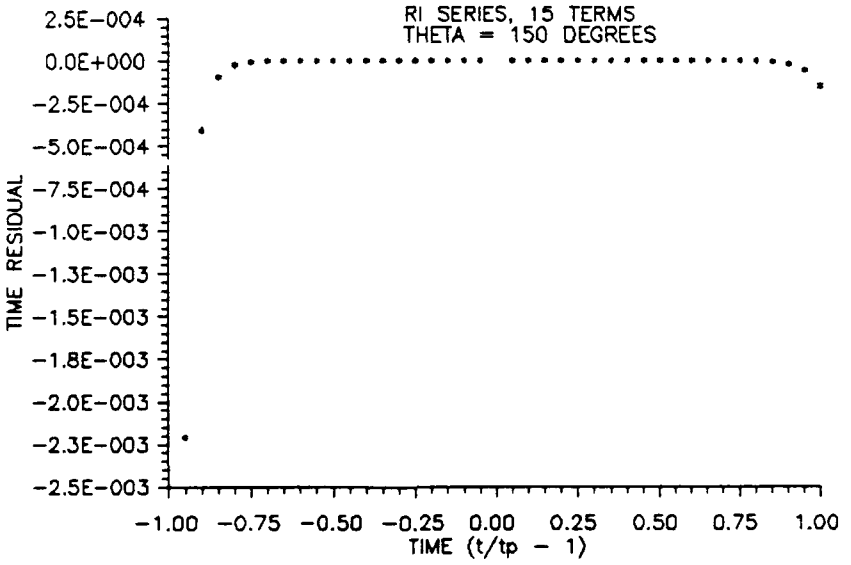

Figure 28b. Time Residual vs. T for a Transfer Angle of 150° Using 15 Terms of the RI Series

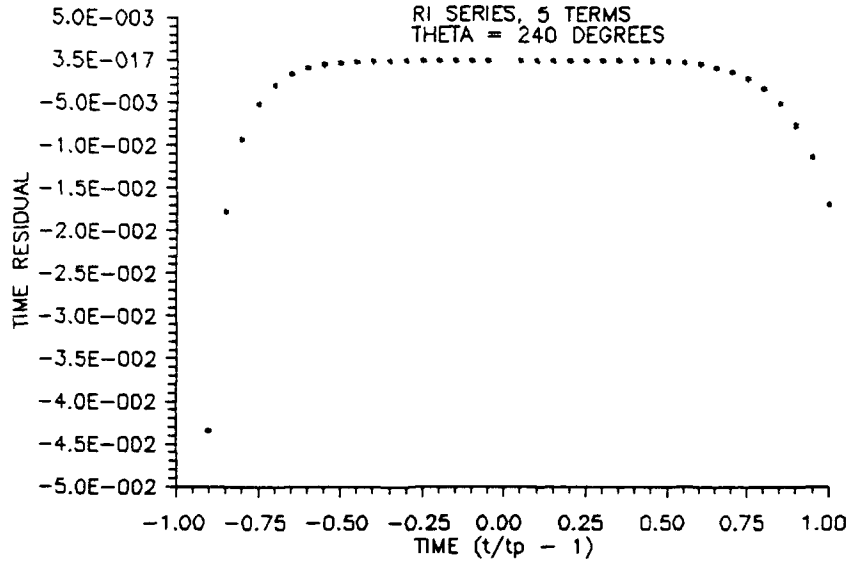

Figure 29a. Time Residual vs. T for a Transfer Angle of 240° Using 5 Terms of the RI Series

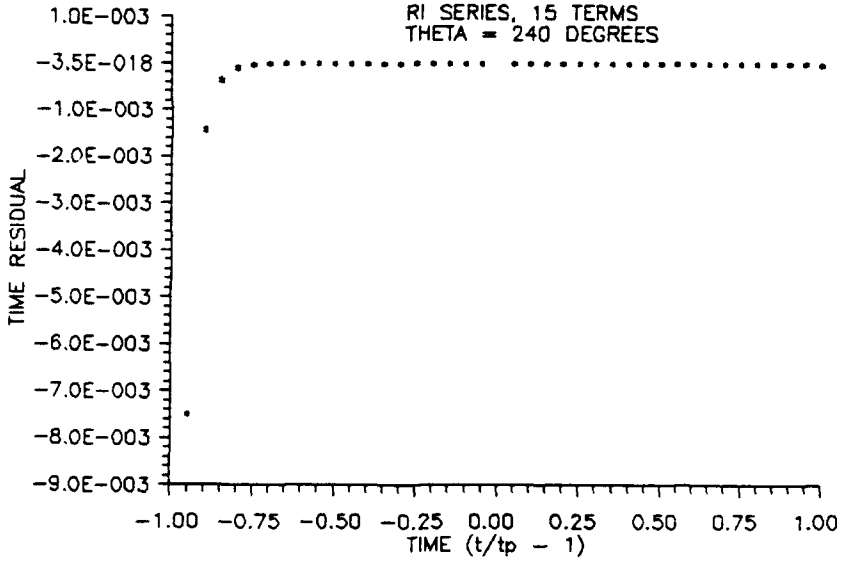

Figure 29b. Time Residual vs. T for a Transfer Angle of 240° Using 15 Terms of the RI Series

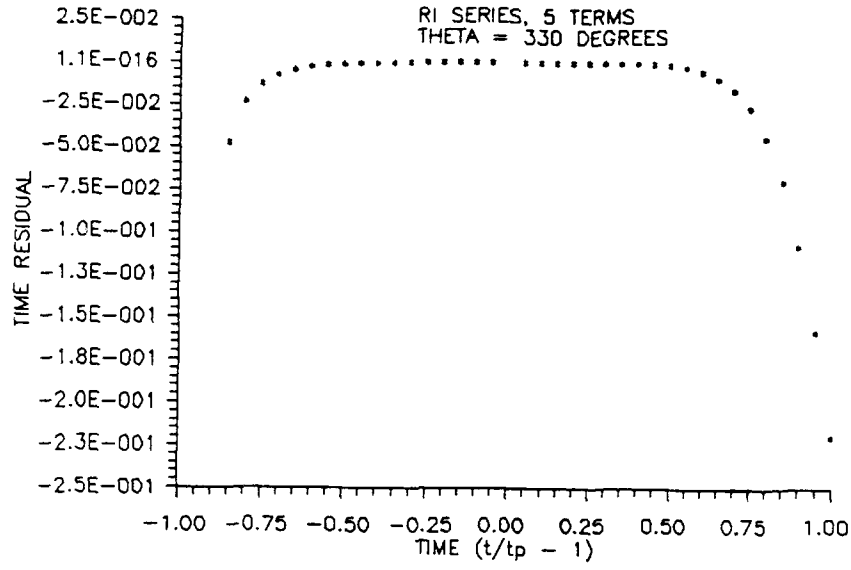

Figure 30a. Time Residual vs. T for a Transfer Angle of 330° Using 5 Terms of the RI Series

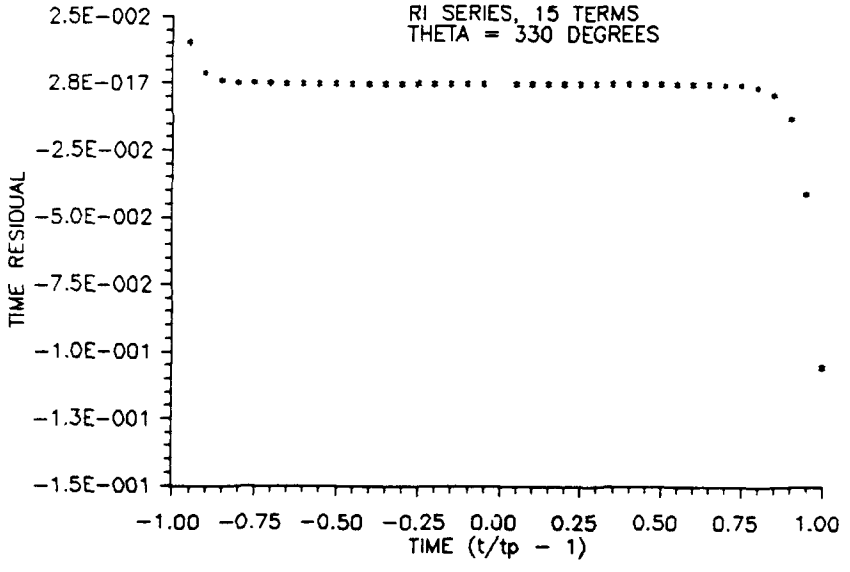

Figure 30b. Time Residual vs. T for a Transfer Angle of 330° Using 15 Terms of the RI Series

Appendix B. *Time Residual vs. T Plots for R Series*

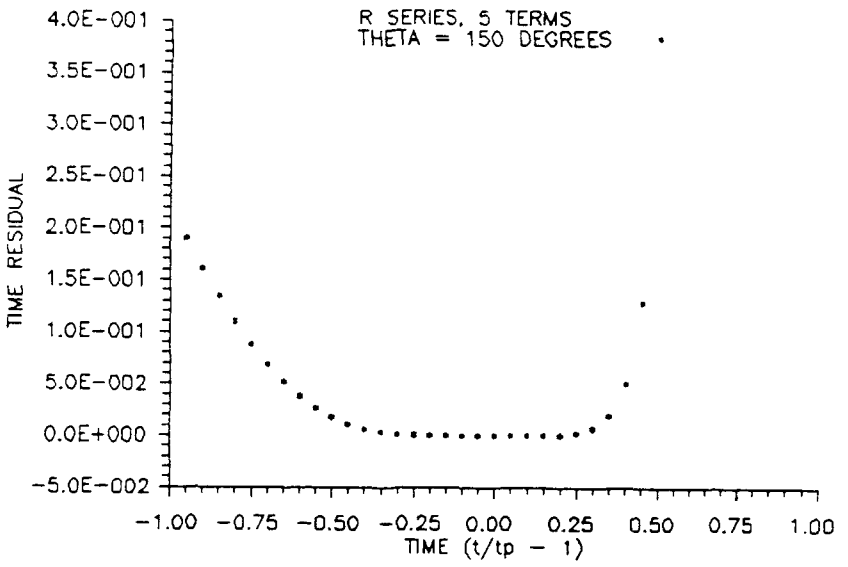

Figure 31a. Time Residual vs. T for a Transfer Angle of 150° Using 5 Terms of the R Series

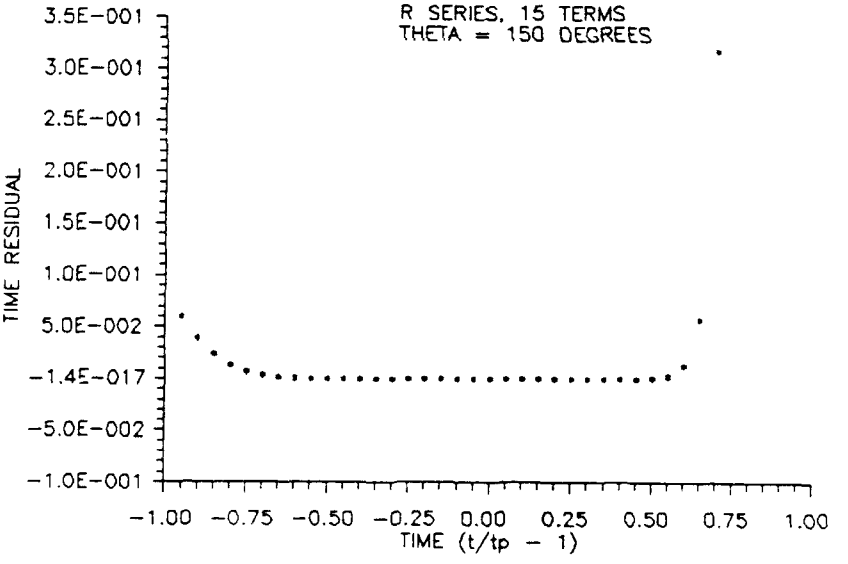

Figure 31b. Time Residual vs. T for a Transfer Angle of 150° Using 15 Terms of the R Series

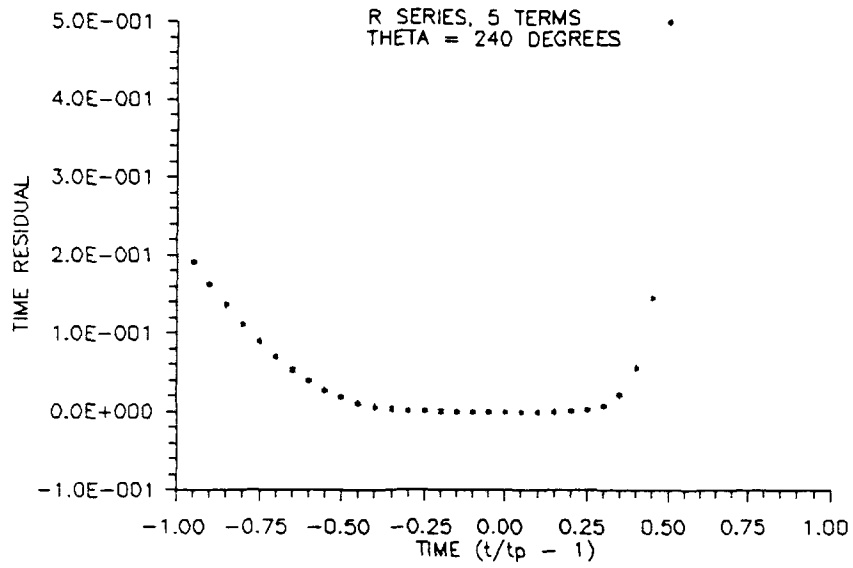

Figure 32a. Time Residual vs. T for a Transfer Angle of 240° Using 5 Terms of the R Series

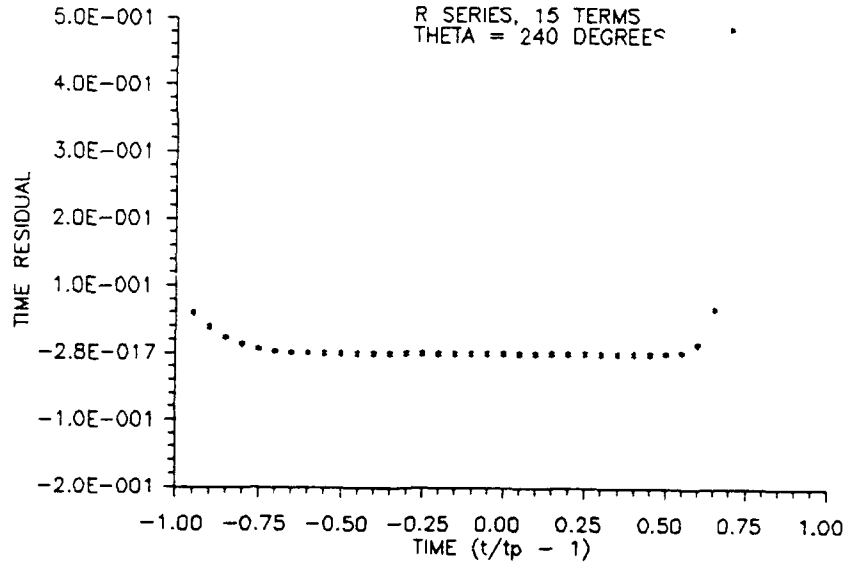

Figure 32b. Time Residual vs. T for a Transfer Angle of 240° Using 15 Terms of the R Series

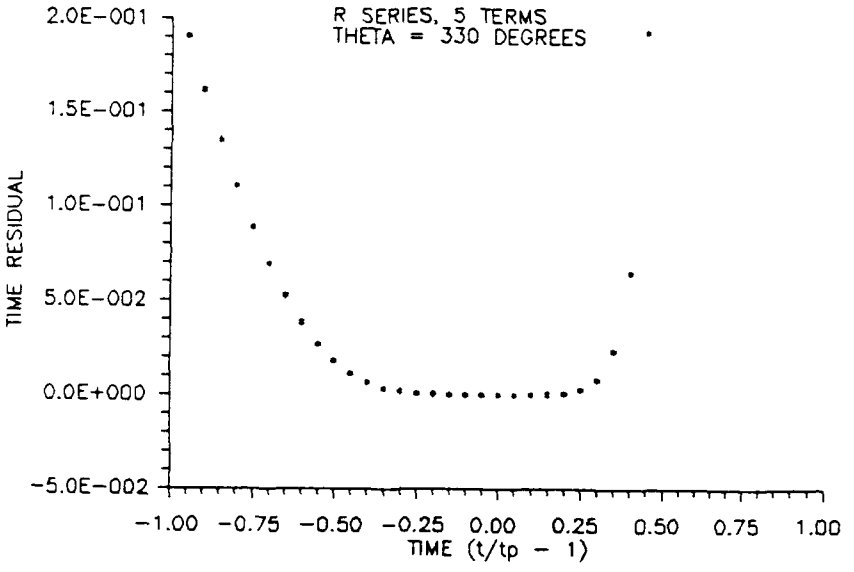

Figure 33a. Time Residual vs. T for a Transfer Angle of 330° Using 5 Terms of the R Series

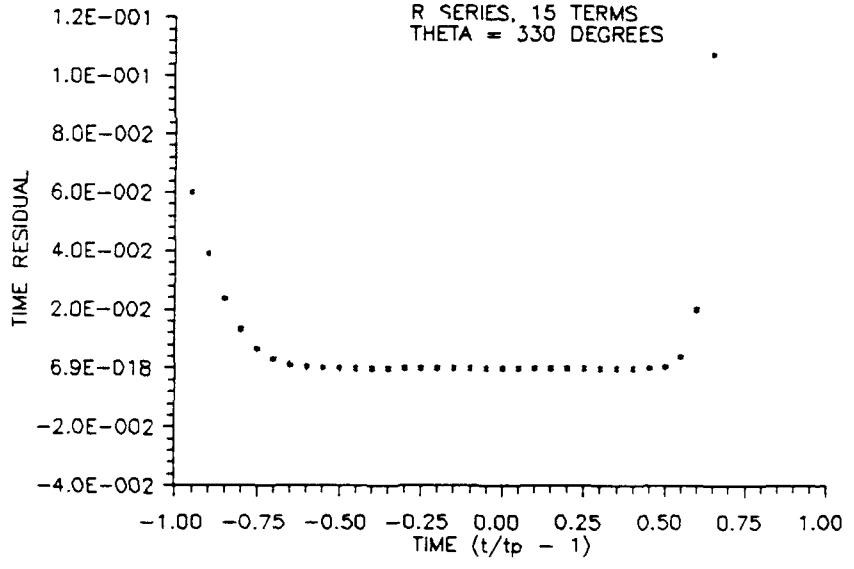

Figure 33b. Time Residual vs. T for a Transfer Angle of 330° Using 15 Terms of the R Series

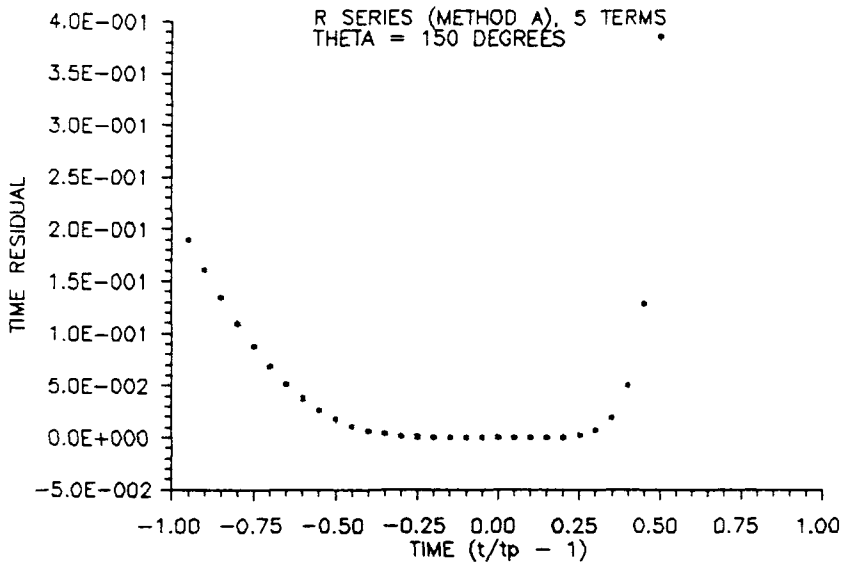

Figure 34a. Time Residual vs. T for a Transfer Angle of 150° Using 5 Terms of the R Series, Method A

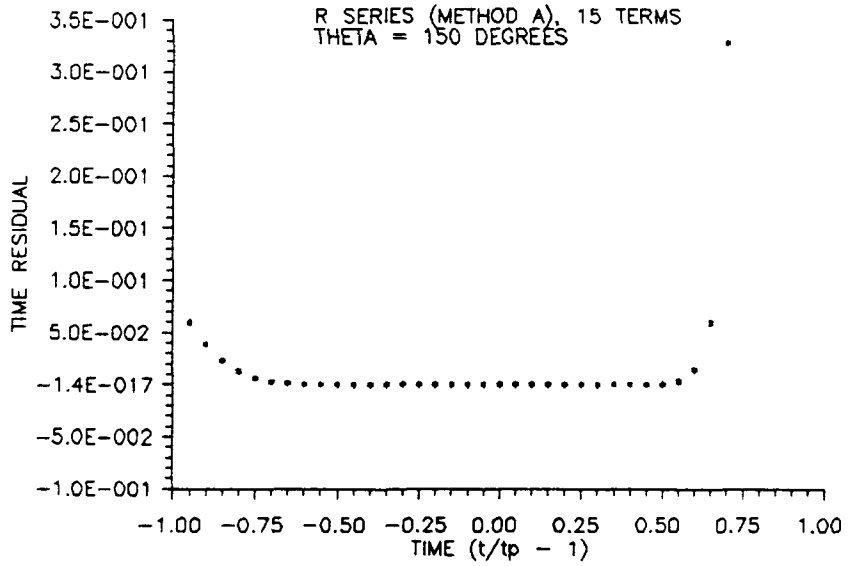

Figure 34b. Time Residual vs. T for a Transfer Angle of 150° Using 15 Terms of the R Series, Method A

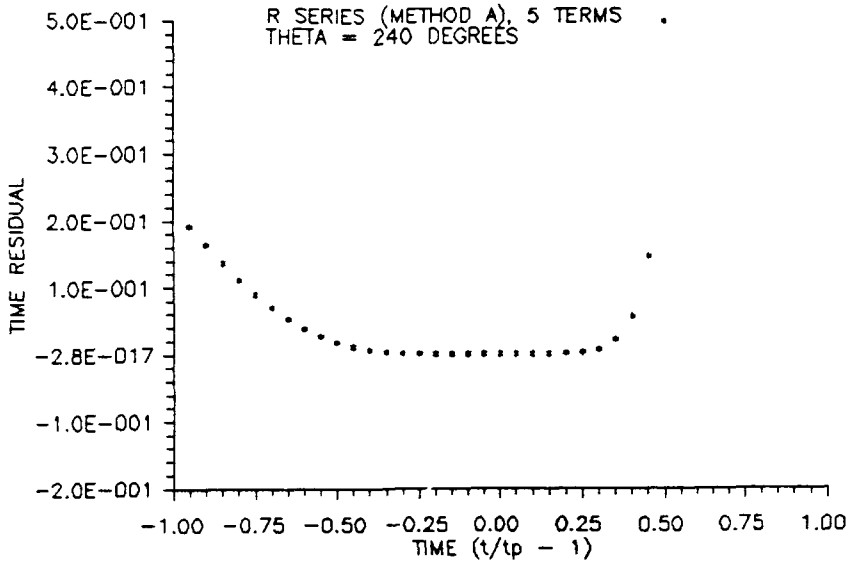

Figure 35a. Time Residual vs. T for a Transfer Angle of 240° Using 5 Terms of the R Series, Method A

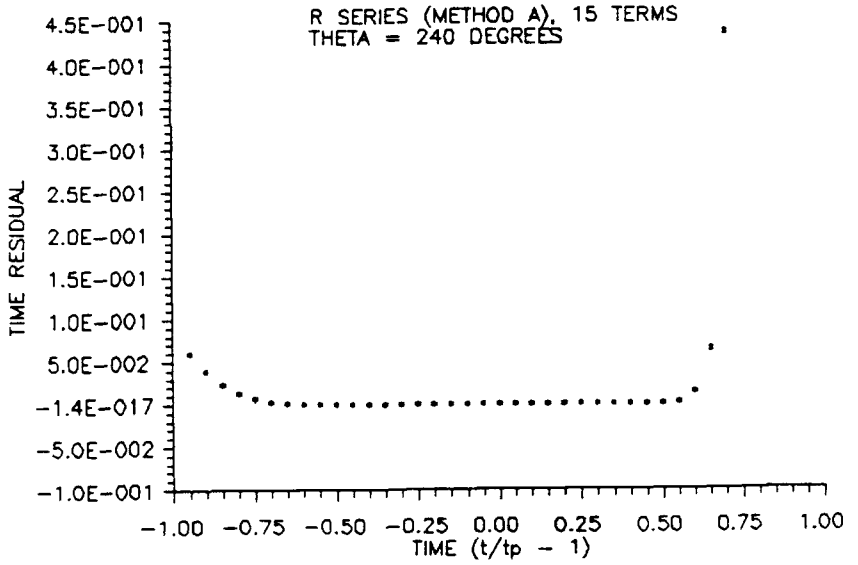

Figure 35b. Time Residual vs. T for a Transfer Angle of 240° Using 15 Terms of the R Series, Method A

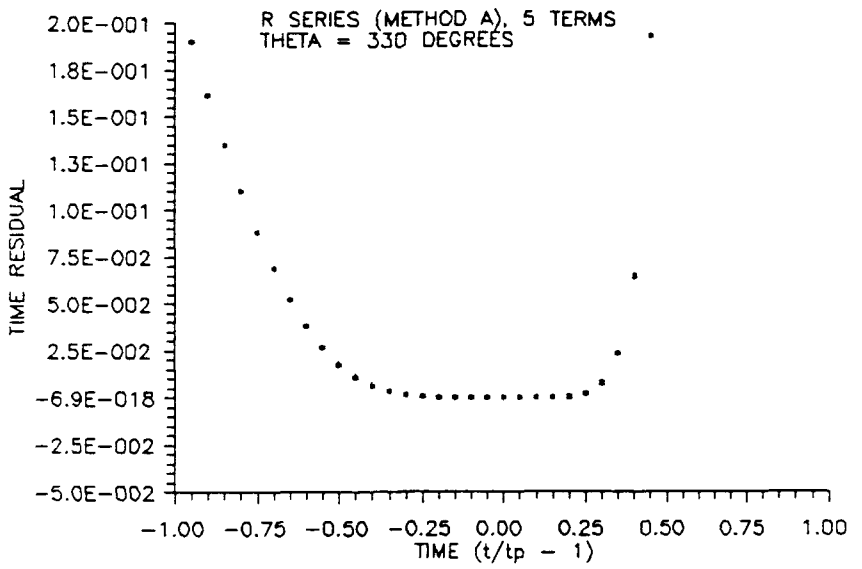

Figure 36a. Time Residual vs. T for a Transfer Angle of 330° Using 5 Terms of the R Series, Method A

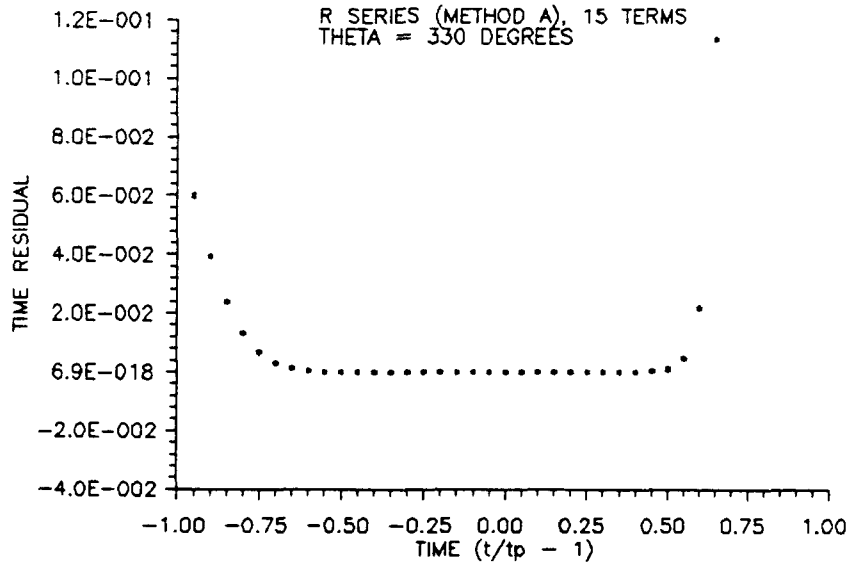

Figure 36b. Time Residual vs. T for a Transfer Angle of 330° Using 15 Terms of the R Series, Method A

Appendix D. *Plots of α_n vs. Transfer Angle*

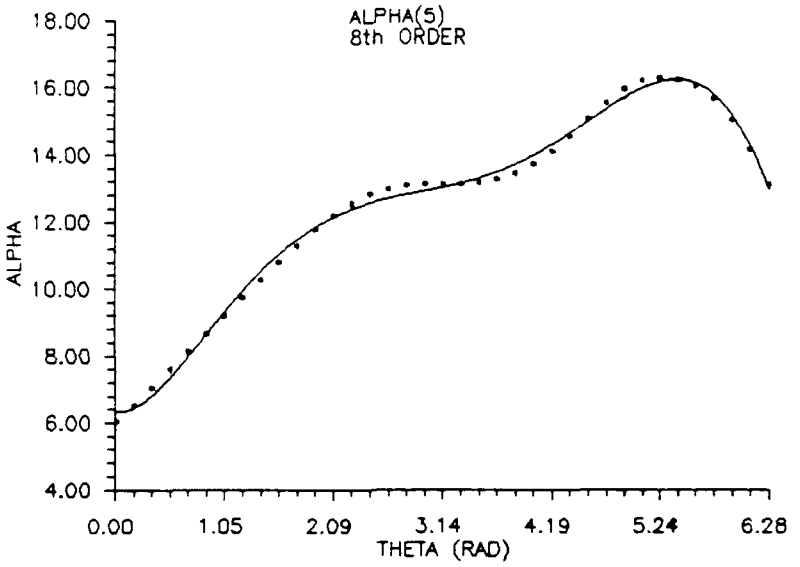

Figure 37a. α_5 vs. Transfer Angle

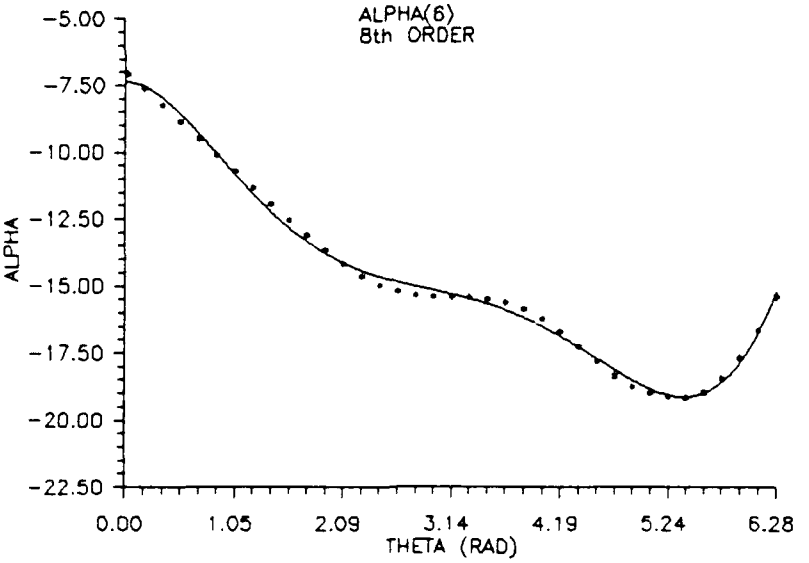

Figure 37b. α_6 vs. Transfer Angle

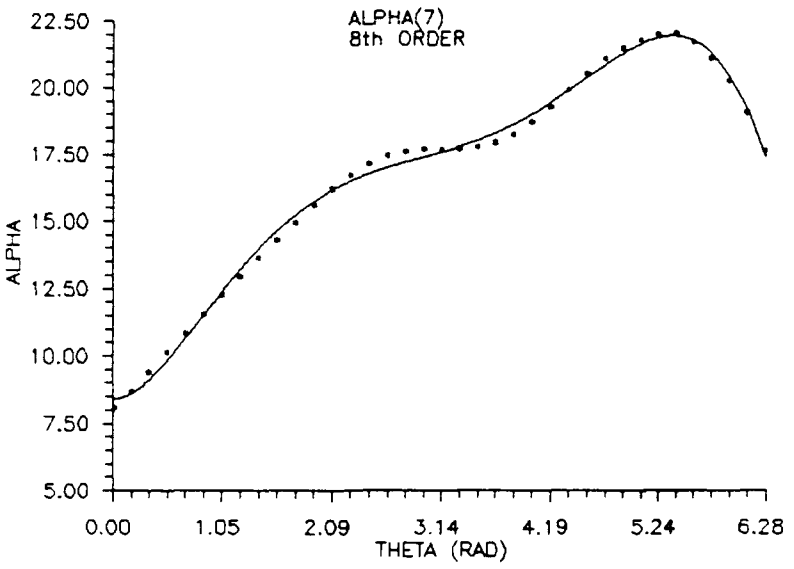

Figure 37c. α_7 vs. Transfer Angle

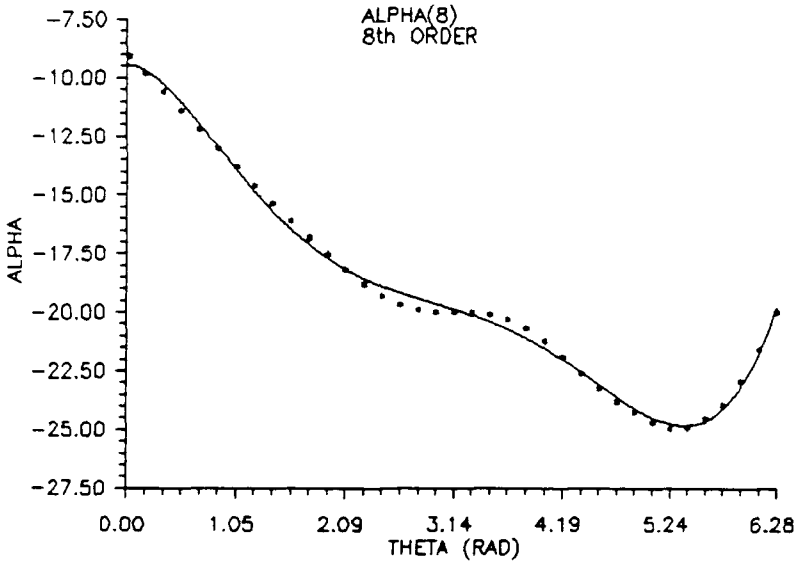

Figure 37d. α_8 vs. Transfer Angle

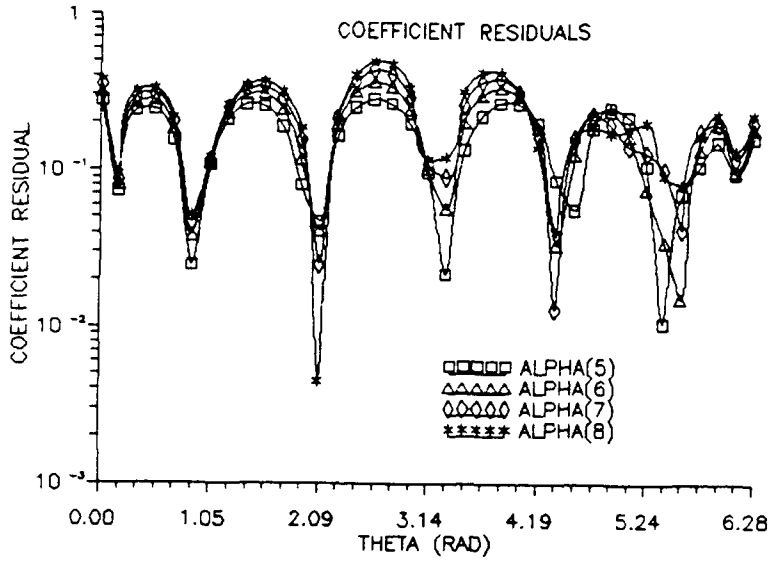

Figure 38. Coefficient Residual vs. Transfer Angle for α_5 through α_8

Appendix E. *Time Residual vs. T Plots for Method B*

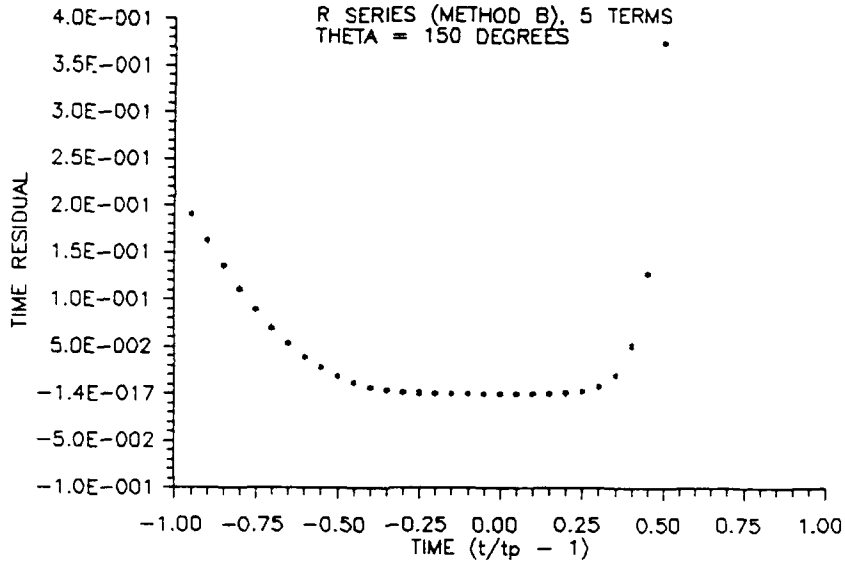

Figure 39a. Time Residual vs. T for a Transfer Angle of 150° Using 5 Terms of the R Series, Method B

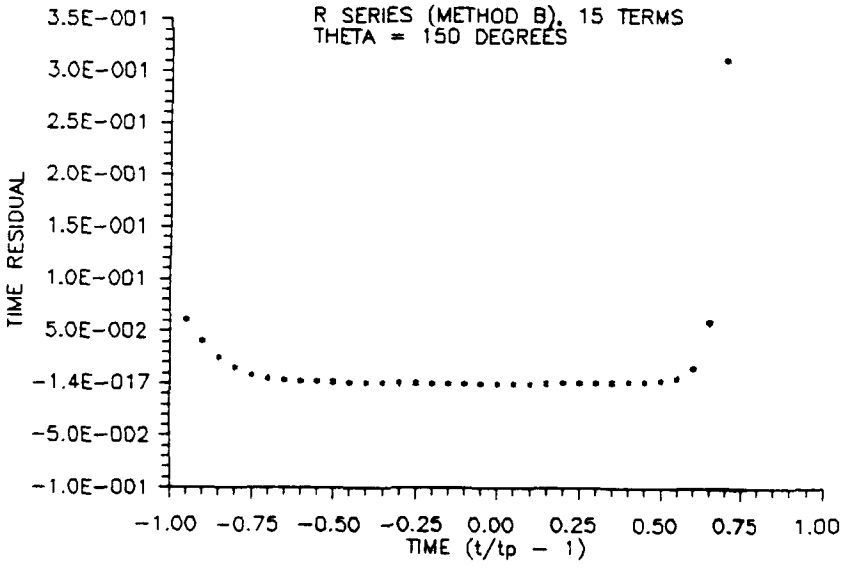

Figure 39b. Time Residual vs. T for a Transfer Angle of 150° Using 15 Terms of the R Series, Method B

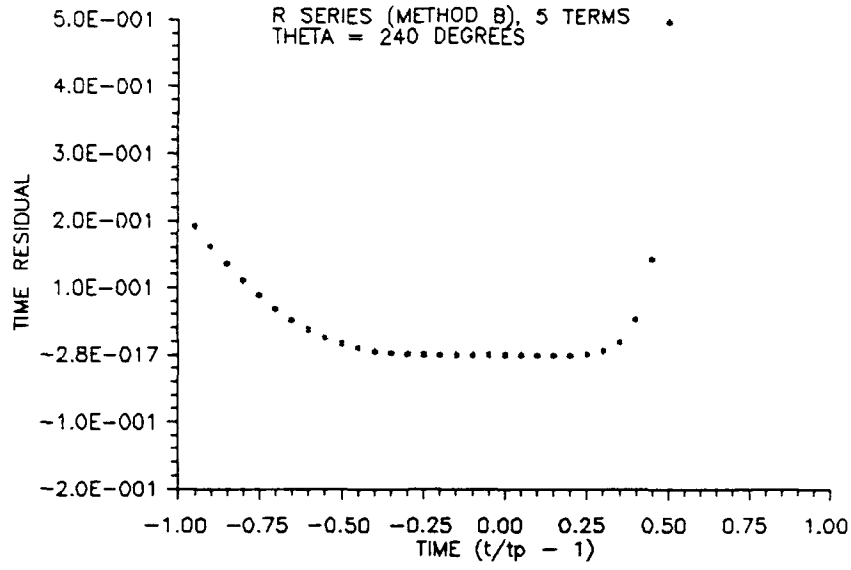

Figure 40a. Time Residual vs. T for a Transfer Angle of 240° Using 5 Terms of the R Series, Method B

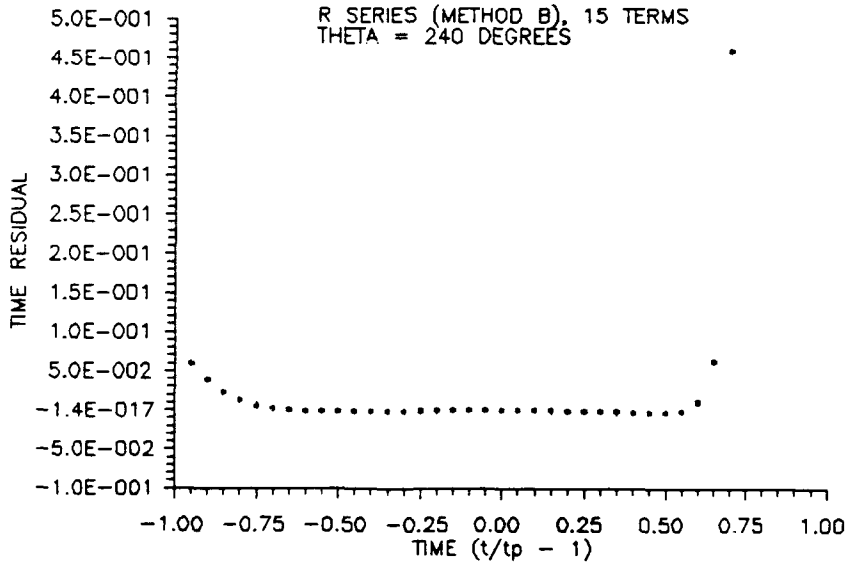

Figure 40b. Time Residual vs. T for a Transfer Angle of 240° Using 15 Terms of the R Series, Method B

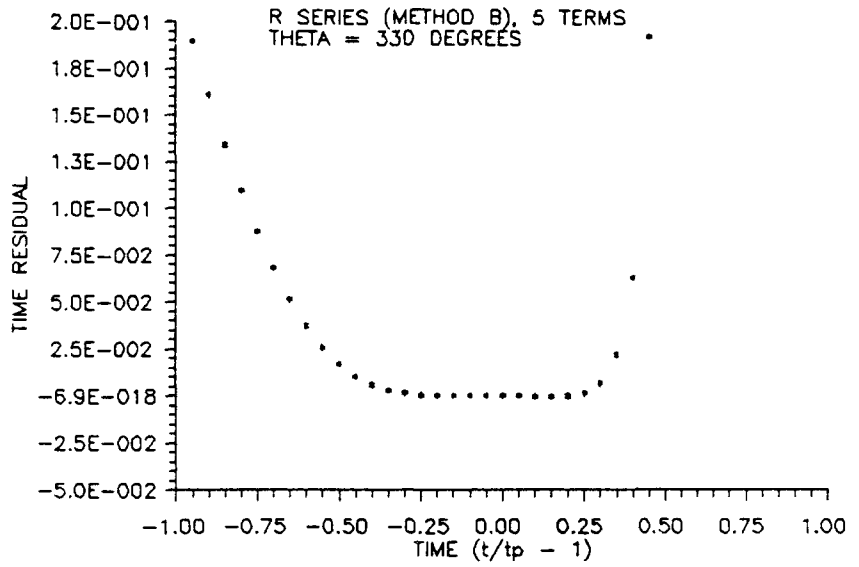

Figure 41a. Time Residual vs. T for a Transfer Angle of 330° Using 5 Terms of the R Series, Method B

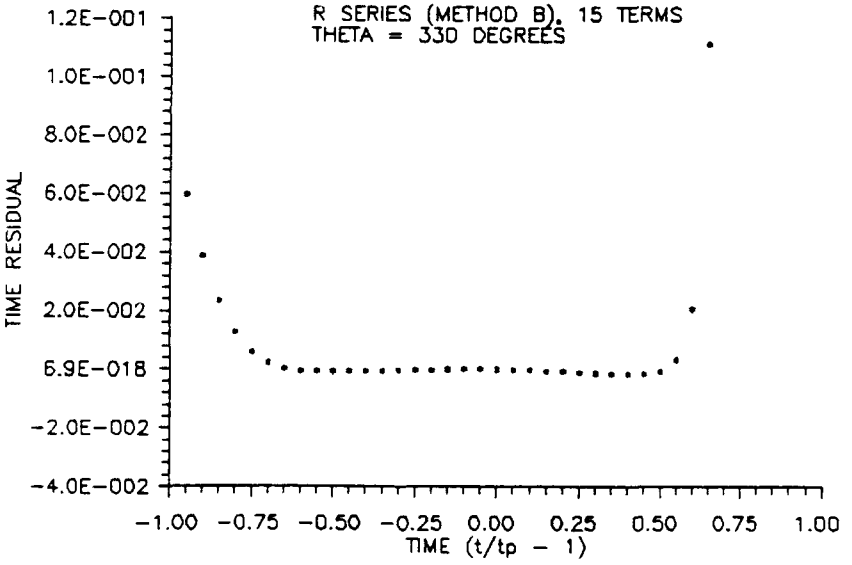

Figure 41b. Time Residual vs. T for a Transfer Angle of 330° Using 15 Terms of the R Series, Method B

Appendix F. *Time Residual vs. T Plots for C. F. Expansion of RI Series*

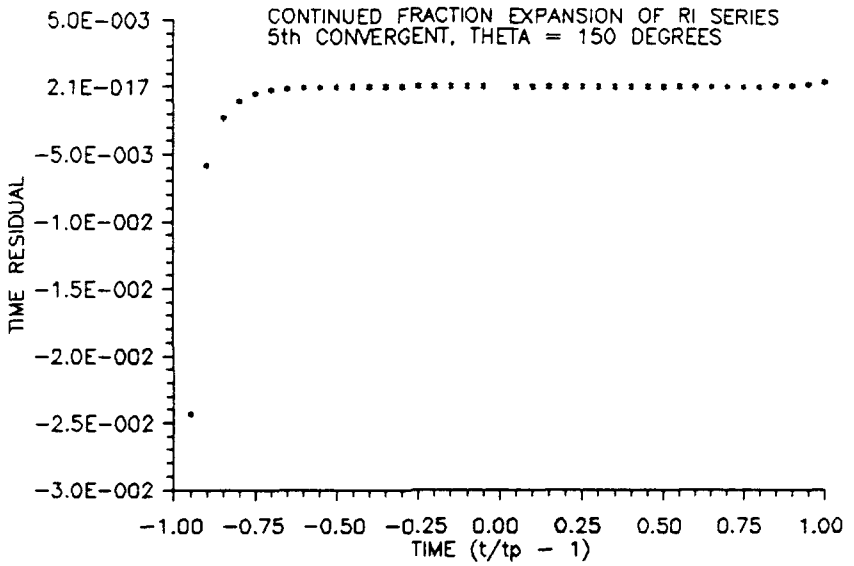

Figure 42a. Time Residual vs. T for a Transfer Angle of 150° Using the 5th Convergent of the C. F. Expansion of the RI Series

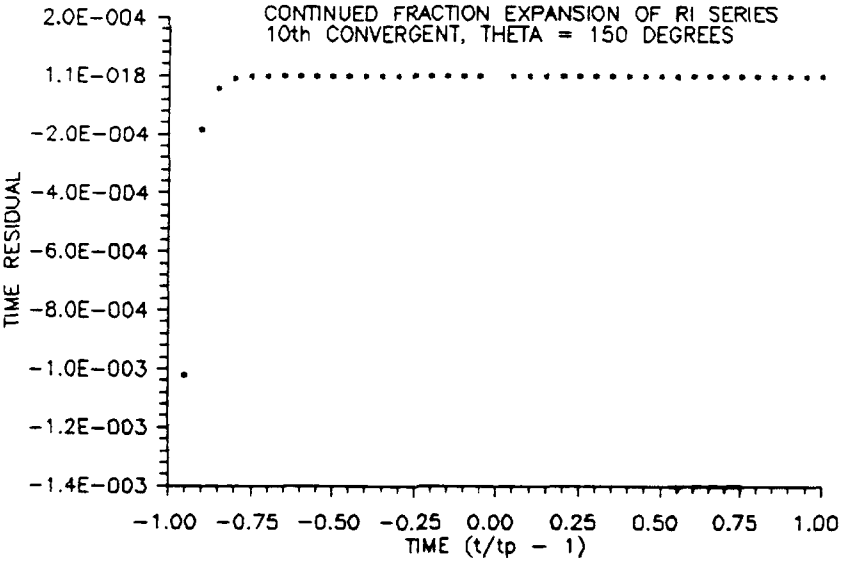

Figure 42b. Time Residual vs. T for a Transfer Angle of 150° Using the 10th Convergent of the C. F. Expansion of the RI Series

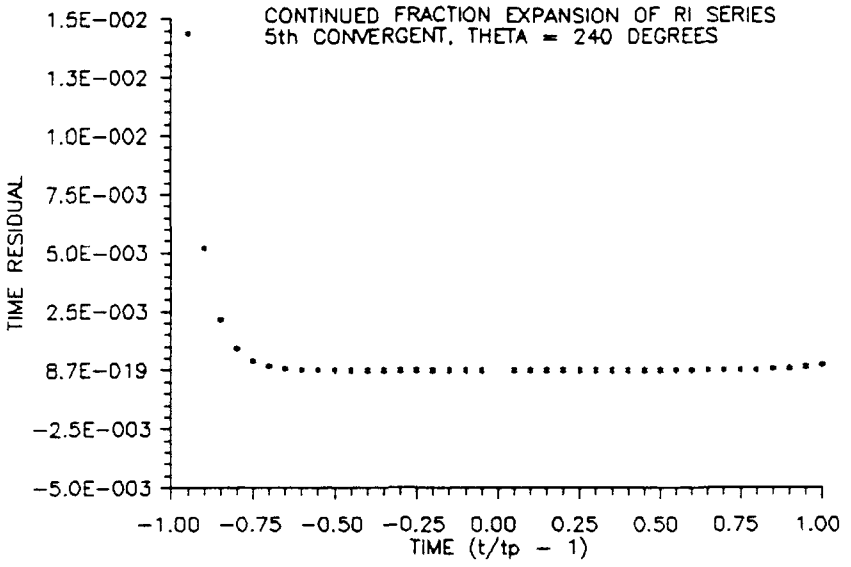

Figure 43a. Time Residual vs. T for a Transfer Angle of 240° Using the 5th Convergent of the C. F. Expansion of the RI Series

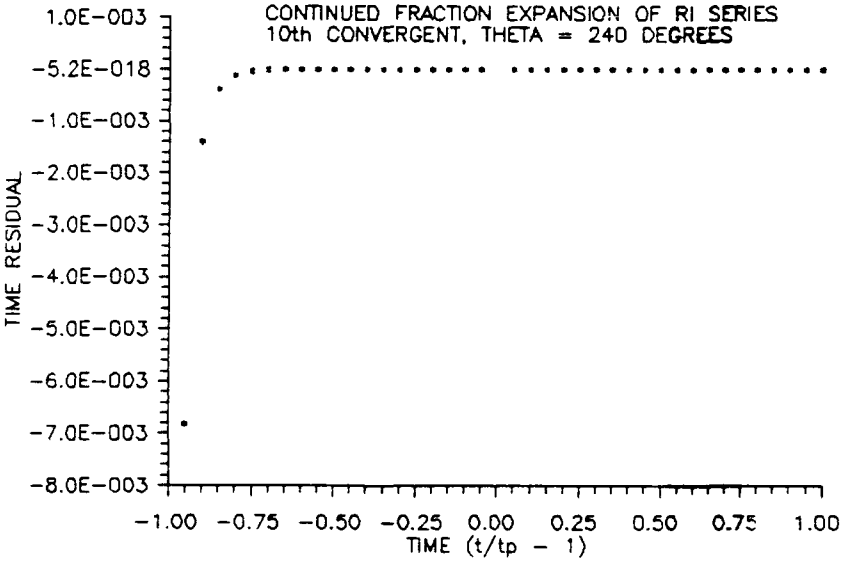

Figure 43b. Time Residual vs. T for a Transfer Angle of 240° Using the 10th Convergent of the C. F. Expansion of the RI Series

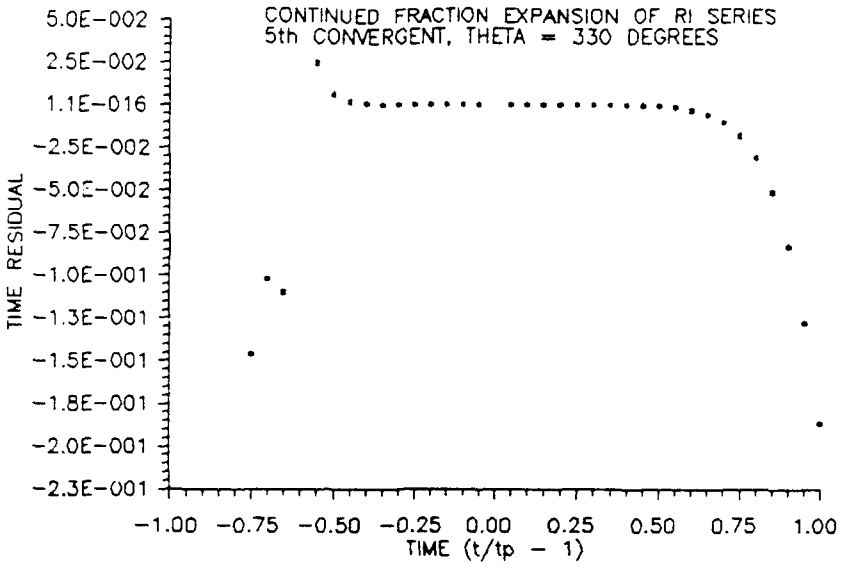

Figure 44a. Time Residual vs. T for a Transfer Angle of 330° Using the 5th Convergent of the C. F. Expansion of the RI Series

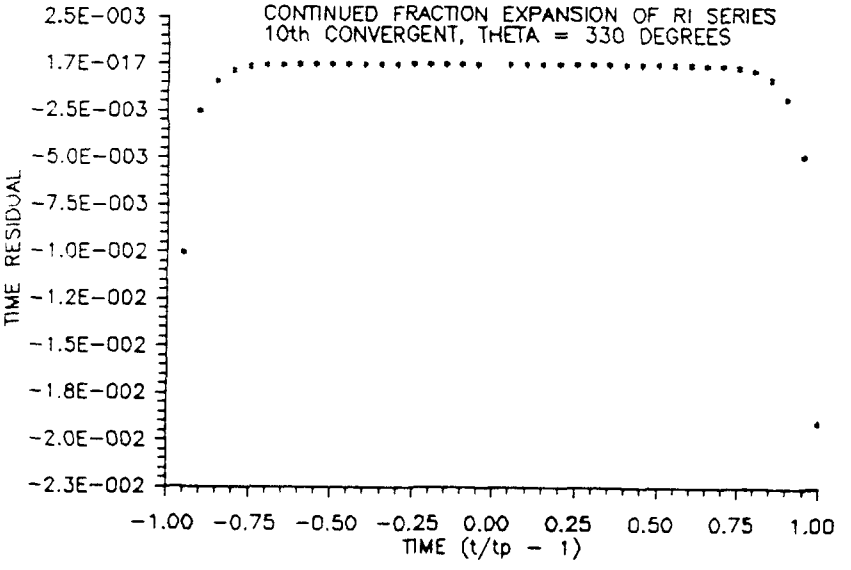

Figure 44b. Time Residual vs. T for a Transfer Angle of 330° Using the 10th Convergent of the C. F. Expansion of the RI Series

Appendix G. *Time Residual vs. T Plots for C. F. Expansion of R Series*

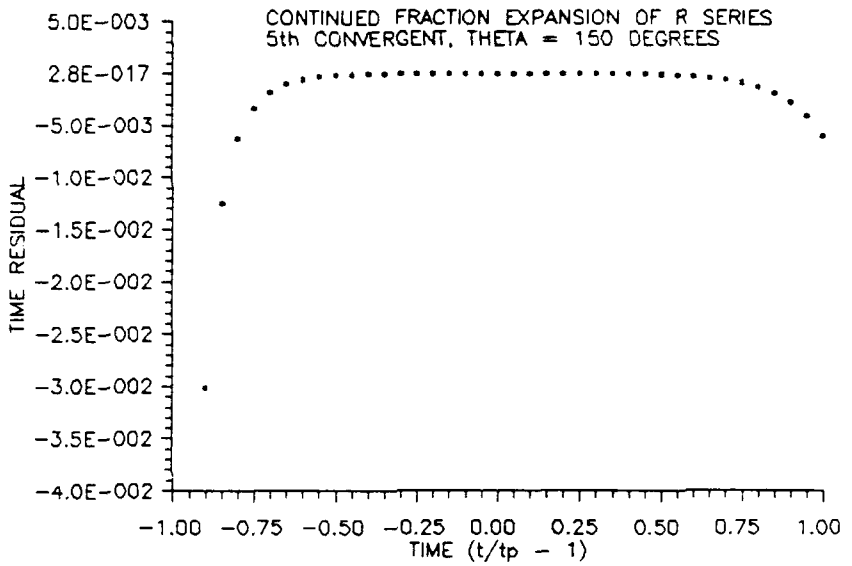

Figure 45a. Time Residual vs. T for a Transfer Angle of 150° Using the 5th Convergent of the C. F. Expansion of the R Series

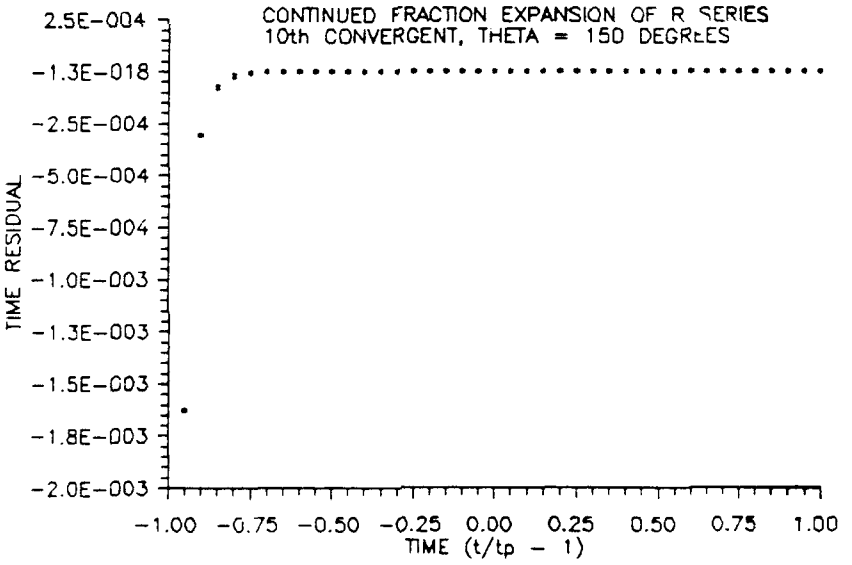

Figure 45b. Time Residual vs. T for a Transfer Angle of 150° Using the 10th Convergent of the C. F. Expansion of the R Series

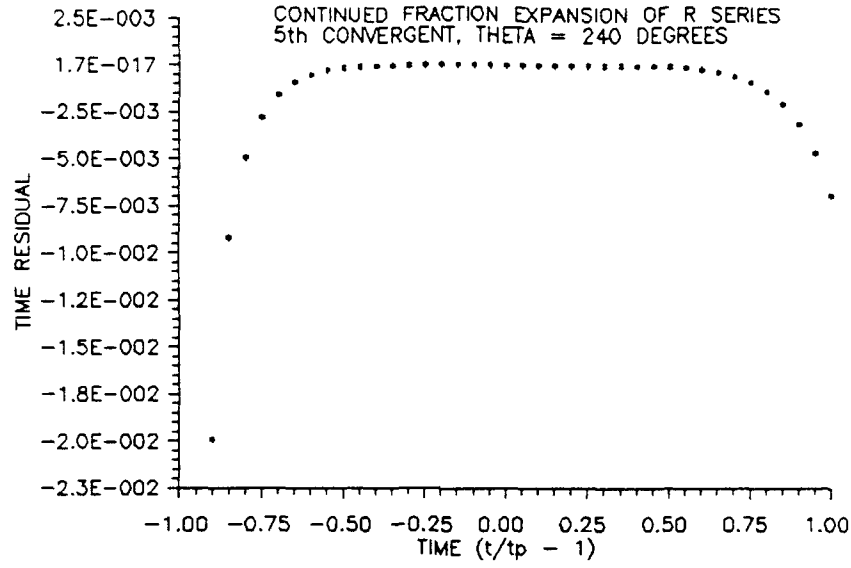

Figure 46a. Time Residual vs. T for a Transfer Angle of 240° Using the 5th Convergent of the C. F. Expansion of the R Series

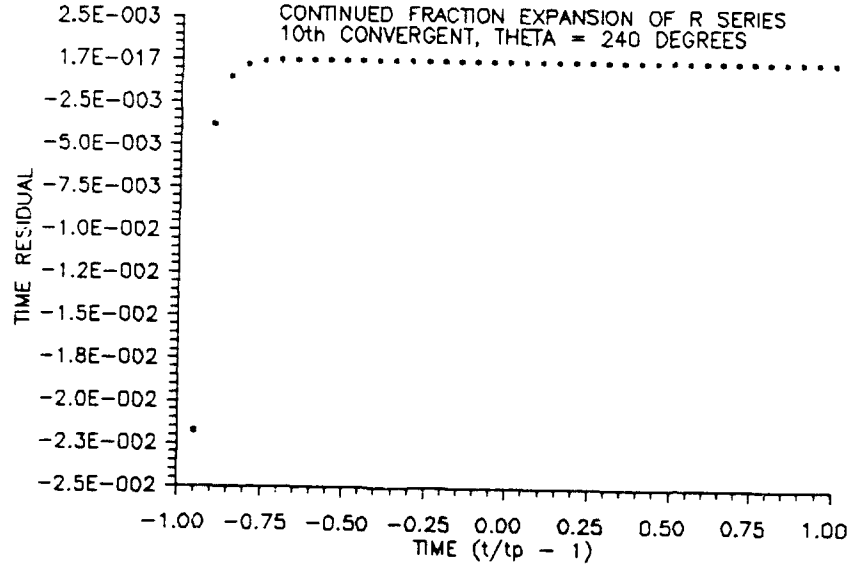

Figure 46b. Time Residual vs. T for a Transfer Angle of 240° Using the 10th Convergent of the C. F. Expansion of the R Series

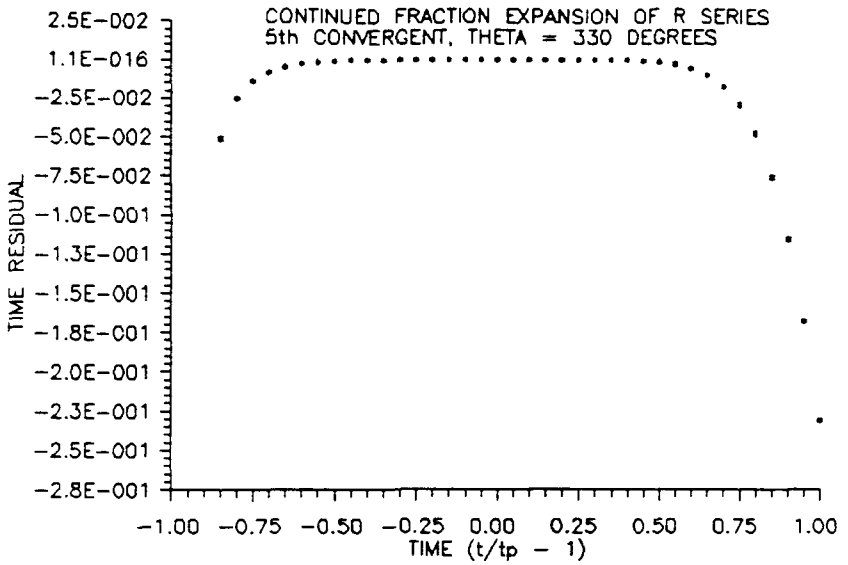

Figure 47a. Time Residual vs. T for a Transfer Angle of 330° Using the 5th Convergent of the C. F. Expansion of the R Series

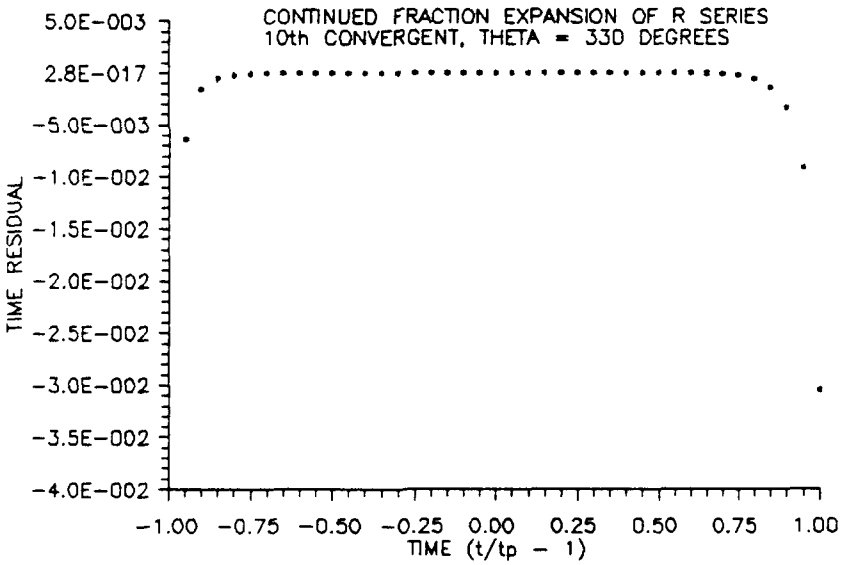

Figure 47b. Time Residual vs. T for a Transfer Angle of 330° Using the 10th Convergent of the C. F. Expansion of the R Series

XIII. Bibliography

1. Bain, Rodney D. MECH 637 Lecture Notes, Air Force Institute of Technology, Summer Quarter 1990.

2. Battin, Richard H. *Astronautical Guidance.* New York: McGraw-Hill Book Company, 1964.

3. -----. *An Introduction to the Mathematics and Methods of Astrodynamics.* New York: American Institute of Aeronautics and Astronautics, Inc., 1987.

4. Thorne, Capt James D. *Series Reversion/Inversion of Lambert's Time Function.* MS Thesis, AFIT/GA/ENY/89D-6. School of Engineering, Air Force Institute of Technology (AU), Wright-Patterson AFB OH, December 1989.

Vita

Captain Michael P. Ward [redacted]

He graduated from Montgomery High School, Santa Rosa CA in 1979. He attended Santa Rosa Junior College for two years then transferred to the University of Oklahoma to pursue a Bachelor of Science degree in Aerospace Engineering. Upon graduation he was commissioned through the AFROTC program on 21 December, 1984. His first assignment was to the Sacramento Air Logistics Center at McClellan AFB, CA where he served as a structural engineer for the F/FB/EF-111 aircraft. While at McClellan AFB he met Laura Barbieri who was a civilian employee at the base. They were married on 10 October 1987. Their son, Christopher, was born on 2 March 1989. In May, 1989 they left sunny California for Wright-Patterson AFB where Michael entered the Air Force Institute of Technology to pursue a Master of Science degree in Astronautical Engineering.

[redacted]

REPORT DOCUMENTATION PAGE

Form Approved
OMB No. 0704-0188

1. AGENCY USE ONLY (Leave blank)	2. REPORT DATE	3. REPORT TYPE AND DATES COVERED
	December 1990	Master's Thesis

4. TITLE AND SUBTITLE
A Numerical Investigation of the Series Reversion/Inversion and Series Reversion of Lambert's Time Function

5. FUNDING NUMBERS

6. AUTHOR(S)
Michael P. Ward, Captain, USAF

7. PERFORMING ORGANIZATION NAME(S) AND ADDRESS(ES)
Air Force Institute of Technology, WPAFB OH 45433-6583

8. PERFORMING ORGANIZATION REPORT NUMBER
AFIT/GA/ENY/90D-14

9. SPONSORING MONITORING AGENCY NAME(S) AND ADDRESS(ES)

10. SPONSORING MONITORING AGENCY REPORT NUMBER

11. SUPPLEMENTARY NOTES

12a. DISTRIBUTION AVAILABILITY STATEMENT
Approved for public release; distribution unlimited

12b. DISTRIBUTION CODE

13. ABSTRACT (Maximum 200 words)

An expression for the semi-major axis as a function of time may be determined by performing a series reversion and inversion of Lambert's Time Function. Since the resulting series contains a singularity, it is desirable to perform only a reversion on the original series to obtain an expression for the inverse of the semi-major axis. Using a Lagrange expansion to obtain the coefficients for this series is very computer intensive. Therefore, alternative methods are presented. Also, each series was expanded into a continued fraction which provided greater accuracy than the series using the same number of coefficients. The accuracy was found to be dependent upon the number of series coefficients used, the transfer time, and the transfer angle.

14. SUBJECT TERMS	15. NUMBER OF PAGES
Orbits, Transfer Trajectories, Celestial Mechanics, Series Reversion, Series Inversion	87
	16. PRICE CODE

17. SECURITY CLASSIFICATION OF REPORT	18. SECURITY CLASSIFICATION OF THIS PAGE	19. SECURITY CLASSIFICATION OF ABSTRACT	20. LIMITATION OF ABSTRACT
Unclassified	Unclassified	Unclassified	UL